Final Results for Pionium Lifetime Measurement with 2001 Data

A. Romero[1], B. Adeva[1], J.L. Fungueiriño Pazos[1], O. Vázquez Doce[1,2],

[1] *IGFAE, University of Santiago de Compostela, Spain*

[2] *INFN, Istituto Nazionale di Fisica Nucleare, Frascati, Italy*

Abstract

Our recent experimental studies of K^+K^- contamination in $\pi^+\pi^-$ sample, together with new Monte Carlo data with improved statistics and angular coverage, as well as consideration of Ni target impurity, have led us to the implementation of a complete set of small corrections to our previous result for Pionium lifetime with 2001 data. Further checks have also been made on the fit stability against various χ^2-fit parameter values.

DIRAC internal note 2007 *25 May 2007*

1 K^+K^- background

Since the publication of our measurement of Pionium lifetime [1], we have investigated experimentally the possible presence of missidentified K^+K^- pairs in the $\pi^+\pi^-$ sample. Although the level of such contamination was expected to be very small [2], its importance stems from the fact that the Coulomb interaction is much stronger for K^+K^- than it is for $\pi^+\pi^-$, at the same value of Q. This is a consequence of the different Bohr radius in the Sommerfeld wave function (so called Sakharov factor $A_C(Q)$). Our investigation proceeded in two steps. First, we determined the contamination fraction $r_K = K^+K^-/\pi^+\pi^-$ at low pair momentum ($p = 2.8\ GeV/c$) to be $r_K = (2.38 \pm 0.35) \times 10^{-3}$, by means of the TDC information of upstream detectors [3], using standard physics triggers. Secondly, we performed a new measurement at higher momentum using Λ triggers and high precision time-of-flight measurements from the Vertical Hodoscopes [4], which allowed us to determine the momentum derivative of r_K. In order to reach a better understanding of the momentum dependence of the K^+K^- signal, we examined in detail both the production of $K^\pm\pi^\mp$ and the semi-inclusive K^+K^- [4], which we compared with a specific Monte Carlo model, the UrQMD [5]. Very good agreement was found between our DIRAC data and UrQMD, particularly concerning the momentum dependence, as a result of our study. Certainly the result is much more constraining in the former case ($K^\pm\pi^\mp$), where we have very high statistics. It seems that the prediction of the momentum derivative is an easier task for Monte Carlo models than it is the strangeness (s,$\bar{s}$) yield itself. Therefore the extrapolation from $p = 2.9\ GeV/c$ to $p = 6.0\ GeV/c$ seems to be precise and reliable, when UrQMD Monte Carlo is used. In addition, of course, we have our experimental measurement at $p = 4.8\ GeV/c$ which comes to confirm that prediction.

1.1 Monte Carlo simulation of K^+K^- signal

Our basic approach has been to fully simulate the K^+K^- background as function of pair momentum, and include the simulated (Q_T, Q_L) spectrum in our standard χ^2-analysis, as a modification of the Coulomb $\pi^+\pi^-$ spectrum. The term $\alpha_1 n_{CC}$ in expression (1) of reference [1] is replaced by the term $\alpha_1(\epsilon n_{KK} + (1-\epsilon)n_{CC})$ where n_{KK} are the normalized spectra for K^+K^-. The fractions $\epsilon(p)$ are determined from our experimental measurements, which follow the parametrization indicated in Fig. 1, which is taken from reference [4].

Generation of K^+K^- pairs is achieved, in the center-of-mass frame, by means of the standard DIRAC atom pair generador [9] [10] after modification of the

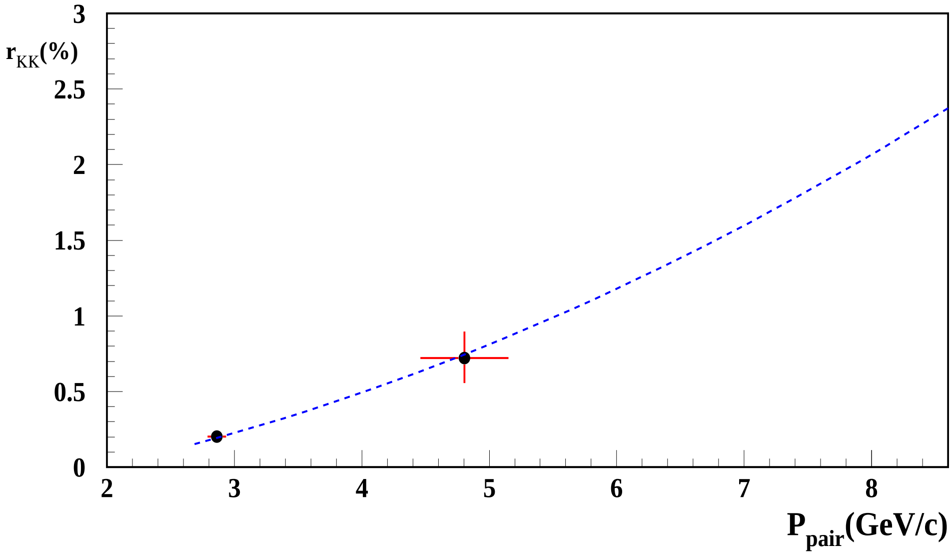

Fig. 1. *Experimental measurements by DIRAC of the $K^+K^-/\pi^+\pi^-$ ratio r_{KK} at two different values of the average pair momentum, namely 2.9 GeV/c and 4.8 GeV/c. The UrQMD Monte Carlo prediction is shown as the dotted line, multiplied by a factor 0.37.*

Bohr radius in the Coulomb factor. Pairs are then boosted into the DIRAC laboratory frame.

It should be noted that the experimental values of Q determined by the spectrometer (from the ARIANE program) are of course calculated under the $\pi^+\pi^-$ hypothesis, and are subject to the standard kinematical cuts implied by the trigger system. As a consequence, the Q range for the center-of-mass generator must actually be enlarged by nearly a factor 4, with respect to the standard trigger cuts, in order to cover completely the spectrometer acceptance. This relativistic consideration enhances, in practical terms, the level of the contamination by nearly that factor.

As we will see in section 3 and 4, the χ^2-analysis shows a significant improvement after the K^+K^- correction.

2 Outline of improved results

2.1 Statistical analysis method

The analysis was carried out following the method described in [1], which is based on a fit to the $2D$ spectrum in (Q_T, Q_L) plane. The χ^2-value is defined by the expression :

$$\chi^2 = \sum_j \frac{\left(N_p^j - \beta(\alpha_1[\epsilon\frac{N_{KK}^j}{N_{KK}} + (1-\epsilon)\frac{N_{CC}^j}{N_{CC}}] - \alpha_2\frac{N_{AC}^j}{N_{AC}} - \alpha_3\frac{N_{NC}^j}{N_{NC}} - \gamma\frac{N_{AA}^j}{N_{AA}})\right)^2}{N_p^j + \beta^2(\alpha_1^2[(1-\epsilon)^2\frac{N_{CC}^j}{N_{CC}^2} + \epsilon^2\frac{N_{KK}^j}{N_{KK}^2}] + \alpha_2^2\frac{N_{AC}^j}{N_{AC}^2} + \alpha_3^2\frac{N_{NC}^j}{N_{NC}^2} + \gamma^2\frac{N_{AA}^j}{N_{AA}^2})} \quad (1)$$

where α_i and γ are the respective Monte Carlo type fractions (according to $\alpha_1 + \alpha_2 + \alpha_3 + \gamma = 1$), β represents the global normalization of the Monte Carlo, which corresponds essentially to the total number of prompt events in the fit region (see section 3.2 for more details). N_p^j, N_{CC}^j, N_{AC}^j, N_{NC}^j, N_{AA}^j are the number of prompt, Coulomb, accidental, non-Coulomb and atom pairs, respectively, in each $2D$ bin, as described in our previous note [1]. Correspondingly, N_p, N_{CC}, N_{AC}, N_{NC}, N_{AA} are total number of events in the fit region.

A **control region** is defined by the domain under the cut $Q_L > 2MeV/c$. We call $Q_L < 2MeV/c$ the **extrapolation region**. Errors are obtained by χ^2 variation of one unit. The fit strategy is to perform a preliminary fit that includes the Pionium Monte Carlo in the linear combination. Then the latter is subtracted and the difference between the prompt and the Monte Carlo spectrum is analysed in detail, in order to measure the number of atom pairs. The breakup probability is then determined by means of the K-factors [1].

The χ^2-fit is performed either globally, including all statistics, as reported in section 3, or at ten individual pair momentum $600MeV/c$ bins, as will be seen in section 4.

2.2 Improved statistics Monte Carlo

In addition to the previous K^+K^- simulation we have increased the statistics of the Monte Carlo simulation of $\pi^+\pi^-$ pairs (Coulomb, non-Coulomb and Pionium) by nearly a factor of three, in this new note. The most CPU-intensive part of this simulation is the generation of the GEANT-DIRAC buffer files. The main motivation for doing this is to reduce even further the

Monte Carlo contribution to the statistical error [1]. As part of this effort, we have also enlarged slightly the azimuthal coverage of the pion pairs that impinch the spectrometer, in order to have a more precise statistical description at the edges of the B-field, from $(\phi_{min}, \phi_{max}) = (1.40\ mrad, 1.74\ mrad)$ to $(1.34\ mrad, 1.79\ mrad)$. Please note that the real B-field map is parametrized by GEANT-DIRAC, and a better simulation might improve the lowest and highest momentum bins. A detailed study of the momentum acceptance of the spectrometer, which we used as a guideline, has been presented in reference [11]. The material budget of upstream detectors was kept to the precise values provided by our 1.5% measurement [12]. A recent study [13] has confirmed qualitatively our results, although with unknown error assesment.

2.3 Q_L acceptance correction

In fact, none of the p-dependent Q_L or Q_T Monte Carlo spectra actually experienced any appreciable systematic change, as a result of this simulation effort, and only statistical fluctuations were observed. The newly simulated non-Coulomb pairs motivated a new fit of the Q_L acceptance functions, based on the same accidental pair data sample from the spectrometer as before, which is given in Fig. 2, where χ^2-values were slightly improved with respect to our previous work. As it can be appreciated, fit quality is sufficiently good in all cases, given the fact that the full statistics of accidental pairs has been used for 2001, along with the very high Monte Carlo statistics. Please note that, after this correction, prompt pairs can be compared with Monte Carlo with no "a priori" knowledge of Coulomb interaction.

The p-dependent Q_L acceptance functions in Fig. 2 were not only used in the momentum dependent fits of section 4, but also in the global fit analysis reported in next section.

2.4 Target impurity correction

We analysed the existing data from the collaboration concerning measurements, as well as calculations, of the effect on the breakup probability of the small impurity of the Ni target foil, from elements of lower Z values [6]. This work was used as the basis to perform a small (positive) correction to the lifetime, which had not been done before in our analysis.

For the sake of easy comparison, we present our correction by quoting the breakup probabilities (P_{Br}) that would have been obtained in a pure Ni target. An identical result for the Pionium lifetime would be obtained, of course,

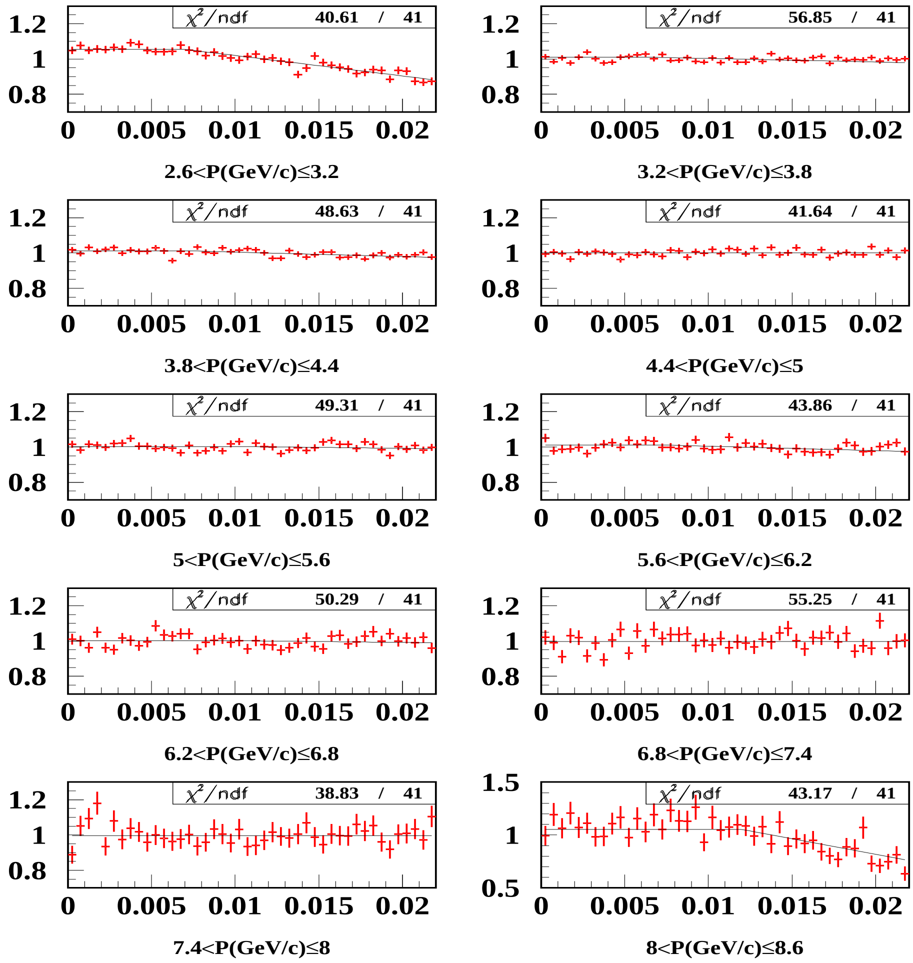

Fig. 2. *Q_L spectrum of the ratio between accidental pairs from the spectrometer and non-Coulomb Monte Carlo, in ten 600 MeV/c bins of lab-frame pair momentum p. The line shows a parametric fit to the data, which was used as a correction for the prompt pairs. Fit χ^2-values are indicated.*

if we retained our unambiguous measurement of P_{Br} and used the Pionium propagation code in a contaminated target.

In order to check a possible dependence of the P_{Br} correction on the pair momentum p, a simulation was done using the propagation code [9] having Al as target foil material. The ratio between the two was plotted as function of p, and the observed slope was $0.05/GeV$. Given such small value, we consider a sufficiently good approximation to apply the same correction factor (1.014) in all momentum bins. When the experimental function $P_{Br}(p)$ is re-fitted to the Monte Carlo prediction, a lifetime increase $\Delta\tau = +0.10\ fs$ is generically observed, very weakly dependent on the status of other corrections.

3 Global fit analysis

3.1 K-factors calculation

The introduction of the new Monte Carlo with improved angular coverage and increased statistics has made us re-calculate the K-factors, which are given in table 1 for the p-integrated case. Also the p-dependent K-factors were re-calculated, which are indicated in table 2 for the standard cuts $Q_T < 5MeV/c$ and $Q_L < 2MeV/c$. In neither of the two cases variations with respect to those reported in [1] are significant.

Table 1
Numerical values of K^{th} and K^{exp} as defined in reference [1], obtained for our improved Monte Carlo simulation. Each raw corresponds to a given rectangular cut in (Q_T, Q_L) plane , with $Q_T^c = 5MeV/c$ and $Q_L^c = 2MeV/c$ being the reference cut values. No practical change is observed with respect to earlier values.

$Q_L^{cut}(MeV/c)$	K^{theo}	K^{exp}
0.5	0.4372	0.3008 $\pm$ 0.0006
1.0	0.2389	0.2191 $\pm$ 0.0004
1.5	0.1669	0.1619 $\pm$ 0.0002
2.0	0.1300	0.1275 $\pm$ 0.0002
$Q_T^{cut}(MeV/c)$	K^{theo}	K^{exp}
0.5	3.2457	0.8692 $\pm$ 0.0050
1.0	1.2382	0.6883 $\pm$ 0.0023
1.5	0.6995	0.5311 $\pm$ 0.0013
2.0	0.4674	0.4058 $\pm$ 0.0008
2.5	0.3426	0.3166 $\pm$ 0.0006
3.0	0.2660	0.2523 $\pm$ 0.0004
3.5	0.2147	0.2064 $\pm$ 0.0003
4.0	0.1781	0.1726 $\pm$ 0.0003
4.5	0.1509	0.1471 $\pm$ 0.0002
5.0	0.1300	0.1275 $\pm$ 0.0002

Table 2
K-factors determined in 10 intervals of laboratory-frame momentum, re-evaluated for the new Monte Carlo simulation.

p interval (GeV/c)	$K - factor$
2.6-3.2	0.1140 ± 0.0004
3.2-3.8	0.1197 ± 0.0003
3.8-4.4	0.1258 ± 0.0003
4.4-5.0	0.1314 ± 0.0004
5.-5.6	0.1362 ± 0.0005
5.6-6.2	0.1397 ± 0.0006
6.2-6.8	0.1449 ± 0.0008
6.8-7.4	0.1466 ± 0.0011
7.4-8.0	0.1467 ± 0.0016
8.-8.6	0.1571 ± 0.0033

3.2 Fit results

The global fit consists in minimizing the χ^2 defined in (1) in $2D$ with respect to α_3 (non-Coulomb fraction) and γ parameters, using the momentum-integrated sample. The β , α_2 and ϵ parameters remain fixed in this fit. α_2 is determined by the direct measurement of the accidental pairs fraction from the analysis of the precision time-of-flight spectrum. $\beta = N_p^c/f_c$ where N_p^c is the number of prompt events with $Q_L > 2MeV/c$ (control region) and f_c is the ratio between the number of Monte Carlo pairs in the control region over the total number of Monte Carlo events. This is practically equal to the total number of prompt events N_p. Slight variations in the definition of β will be discussed in subsection 3.3. ϵ is fixed to the K^+K^- fraction determined in section 1.

We have chosen to perform the fit in 0.25×0.25 $(MeV/c)^2$ bins in the (Q_T, Q_L) plane. Variations with respect to this choice will be reported next. Once the fit has converged, we define the atom signal in each (i, j) bin as the difference between the prompt spectrum (with accidentals subtracted as explained before) and the Monte Carlo with the Pionium component (AA) removed. This 2D signal, which reveals the excess with respect to the calculated Coulomb interaction enhancement, is what we call the Pionium spectrum. The atom breakup probability P_{br} is then determined by means of the K-factors.

Along with the other topics, we have addressed in this note the sensitivity of the data to the finite-size correction [8]. In order to report the contributions of the various small corrections in a comprehensive way, and to facilitate easy comparison with respect to our previous note [1], we define the correction sequence in a cumulative way, as follows:

a) use improved statistics Monte Carlo.
b) include K^+K^- correction.
c) perform the target impurity correction.
d) remove the finite-size correction.

In table 3 we present the χ^2 values (separately in control and extrapolation regions), the number of atoms N_A, the number of Coulomb pairs in the complete fit range N_{CC}, the β parameter and the P_{br} for each option.

Table 3
Fit results for the correction options a), b), c), d)) indicated in the text. χ^2's in the full domain, and its restriction to the control and extrapolation regions separately, are given. Also the total number of atoms N_A and coulomb pairs N_{CC}, the β parameter and the break-up probabilities are indicated.

	a)	a+b)	a)+b)+c)	a)+b)+c)+d)
${\chi^2}_{tot}/ndf$	1547.2/1600	1544.9/1600	1544.9/1600	1540.4/1600
${\chi^2}_{ext}/ndf$	154.6/160	154.3/160	154.3/160	154.2/160
${\chi^2}_{cont}/ndf$	1392.6/1440	1390.6/1440	1390.6/1440	1386.2/1440
N_A	6424 ± 214	6156 ± 206	6156 ± 206	6257 ± 208
N_{CC}	737887 ± 4729	726280 ± 4651	726280 ± 4651	717476 ± 4598
β	882673.2	882910.6	882910.6	882857.8
P_{Br}	0.423 ± 0.016	0.412 ± 0.015	0.418 ± 0.016	0.428 ± 0.016

Please note that whereas the introduction of the K^+K^- contamination decreases the total χ^2 by 2.3 units, the removal of the finite-size correction decreases it by 4.5 units. The combined effect of both actions decreased the total χ^2 by 6.8 units. In addition, as it can be seen in the figure 8, the introduction of the K^+K^- correction introduces a significantly better stability of the measured P_{Br} values with respect to the Q_T cut (at the very low Q_T end), as compared with our earlier result [1]. We will see in section 5 that both of these results will be confirmed, with even larger significance. As a consequence, we drop the finite-size correction.

As far as the K^+K^- correction is concerned, we have made the exercise of letting the ϵ parameter free in the fit. When this is done, we obtain $\epsilon = 0.010 \pm 0.006$ which is entirely compatible with the value $\epsilon = 0.0072$ used in the fit, determined from our measurement [3].

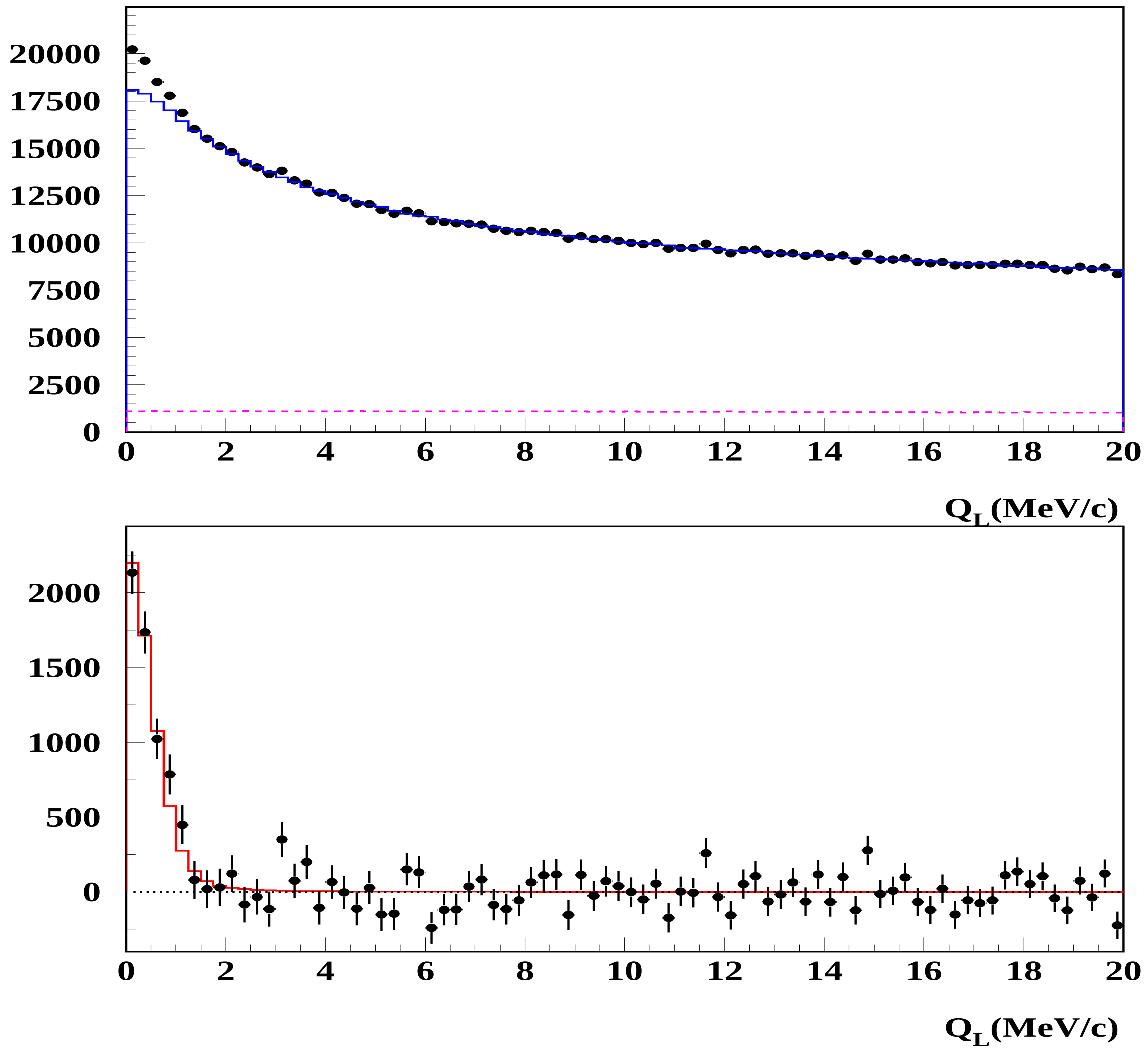

Fig. 3. *Two-dimensional global fit projection onto Q_L. Non-Coulomb background, after subtraction of 8.5 % accidental pairs, is shown as dotted line. The difference between prompt data (dots) and Monte Carlo (blue line) , which corresponds to Pionium signal, is plotted at the bottom, where the signal is compared with the Pionium atom Monte Carlo (red line).*

The Pionium $2D$ signal is shown in the form of lego plots in figures 6 and 7.

3.3 Normalization dependence

We have checked the effect of alternative definitions of the β parameter with respect to the one given above. First, we fixed it to the total number of prompt events in the fit domain, $\beta = N_p$. Secondly, we left it as a free parameter in the

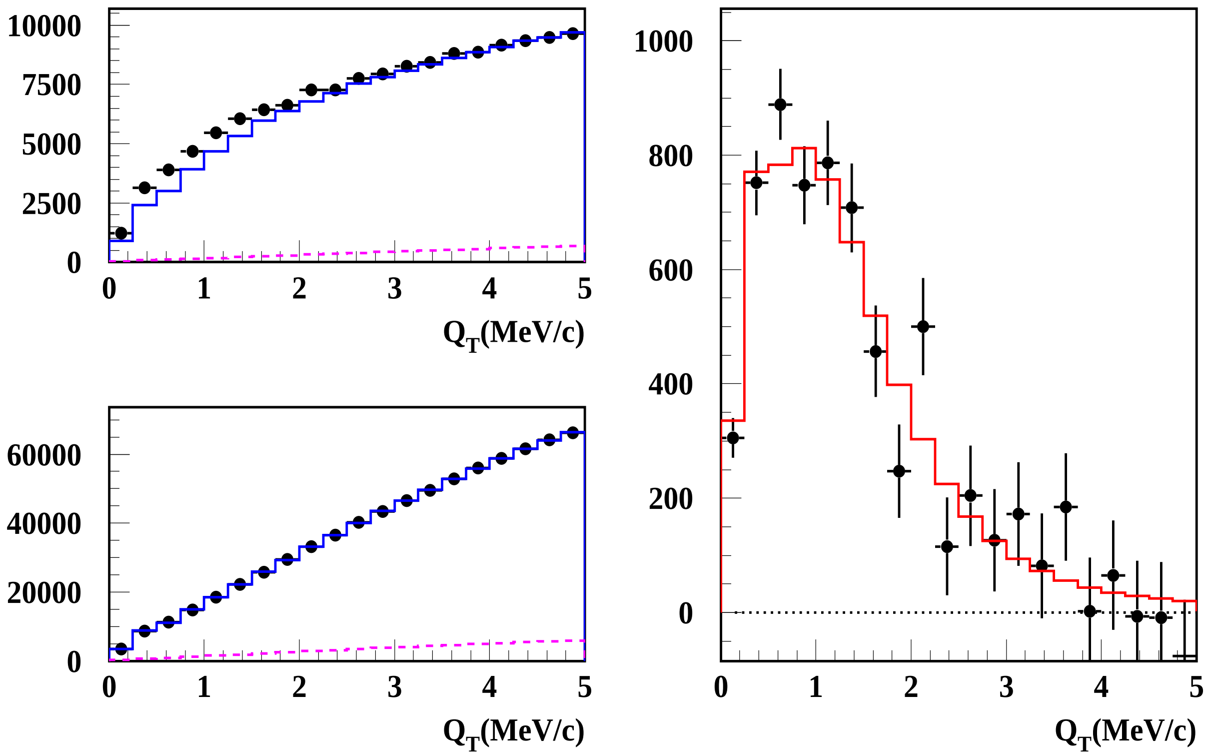

Fig. 4. *Two-dimensional global fit projection onto Q_T. The data are shown separately for $Q_L < 2MeV/c$ (left top) and $Q_L > 2MeV/c$ (left bottom). Non-Coulomb background is also shown as dotted line, after subtraction of 8.5 % accidentals . The difference between prompt data (dots) and Monte Carlo (blue line), which corresponds to transverse Pionium signal, is plotted (right) and compared with the Pionium atom Monte Carlo (red line).*

fit. In table 4 we compare the corresponding values of the breakup probability and also give the explicit values of β (for the full correction set defined above). Variations appear to be within the statistical error.

Table 4
Comparion of global fit results for three different choices of the β parameter definition.

	β	P_{Br}	χ^2/ndf
β all range	883023	0.419 $\pm$ 0.015	1540.7/1600
β ($Q_L > 2MeV/c$)	882858	0.428 $\pm$ 0.016	1540.4/1600
β free	881580	0.435 $\pm$ 0.016	1538.5/1600

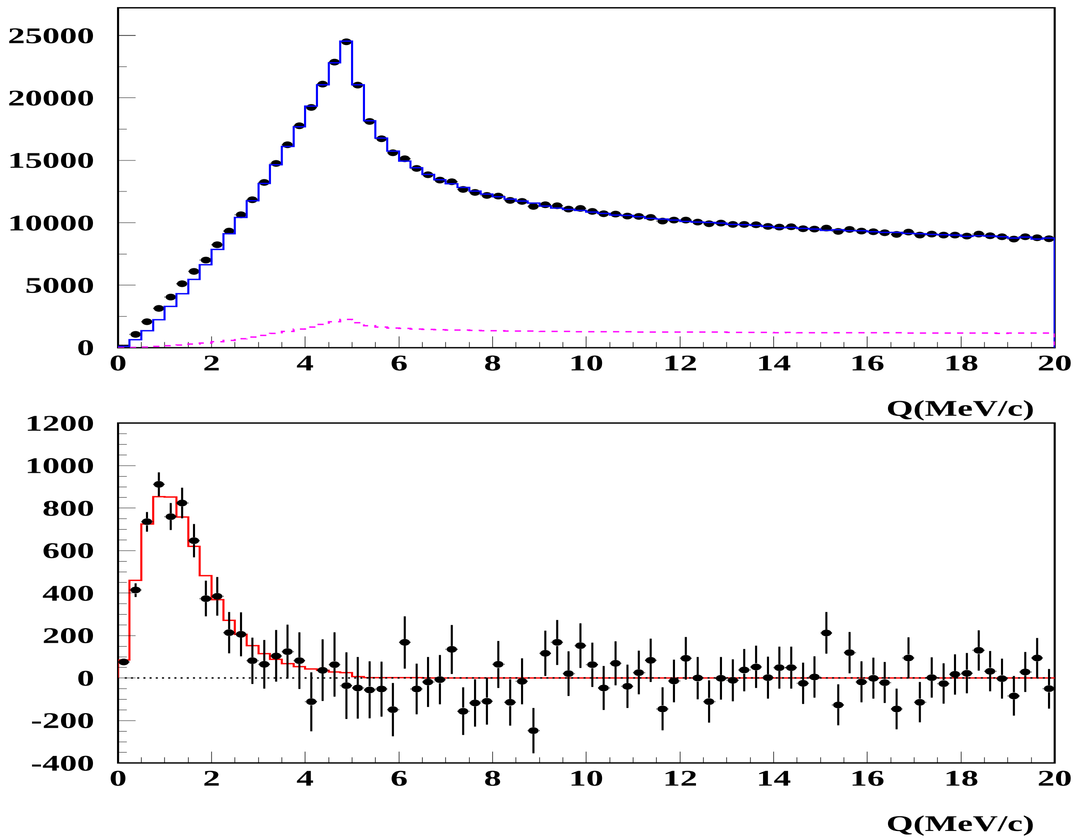

Fig. 5. *Two-dimensional global fit projection onto Q. Non-Coulomb background, after subtraction of 8.5% accidentals, is shown as dotted line. The difference between prompt data (dots) and Monte Carlo (blue line) , which corresponds to Pionium signal, is plotted at the bottom. The signal is compared with the Pionium atom Monte Carlo (red line).*

3.4 Binsize dependence

We also checked the variation of the fit result when we change the 0.25×0.25 $(MeV/c)^2$ binsize to 0.5×0.5 $(MeV/c)^2$. Despite the strong reduction in the number of degrees of freedom, the P_{Br} values remain very similar, as shown in table 5. Note the β parameter has been left free in the fit.

Table 5
Comparison of global fit results using two different (Q_T, Q_L) binsizes.

	β	P_{Br}	χ^2/ndf
0.25×0.25	881580	0.435 ± 0.016	1538.5/1600
0.5×0.5	882654	0.429 ± 0.016	393.2/400

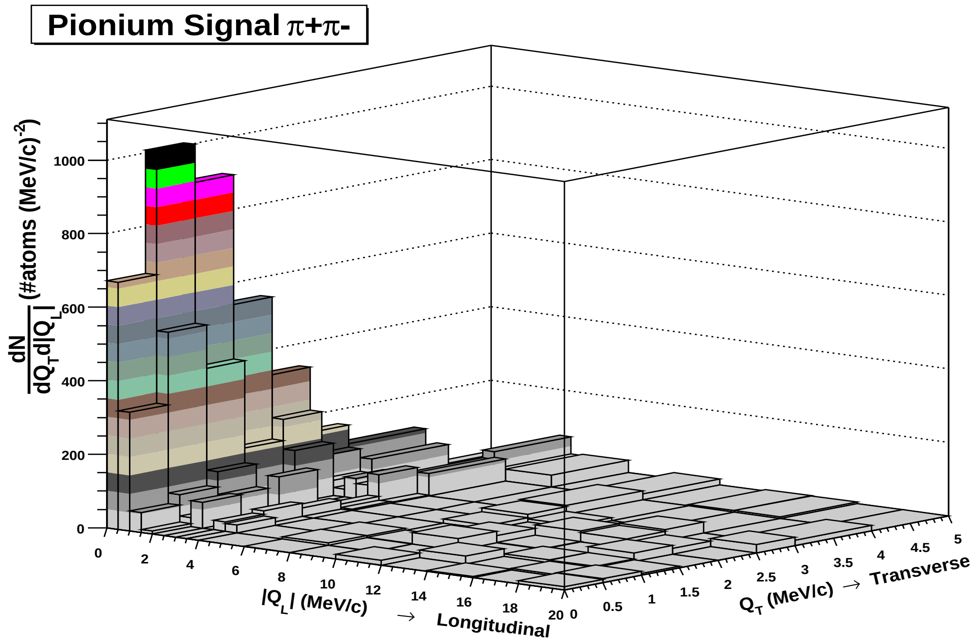

Fig. 6. *Lego plot showing the Pionium break-up spectrum in Ni in the* $(Q_T, Q_L = |Q_Z|)$ *plane, after subtraction of the Coulomb background.*

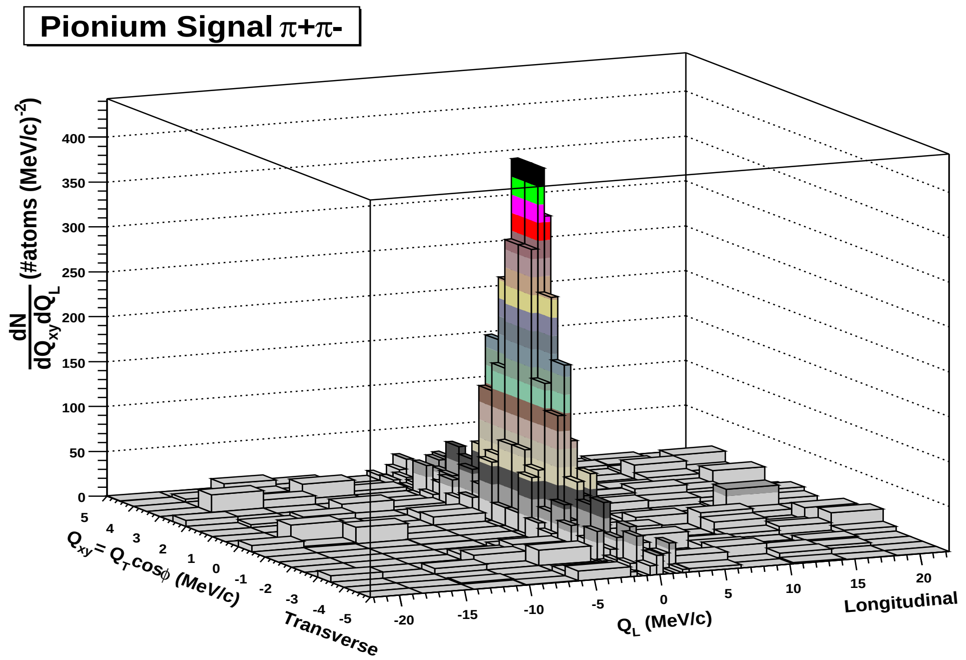

Fig. 7. *Lego plot showing the Pionium break-up spectrum in Ni in the* (Q_{xy}, Q_L) *plane, after subtraction of Coulomb background. The transverse component* $Q_{xy} = Q_T\ cos\phi$ *is defined as the product of the measured* Q_T *value times the cosine of a random azimuth.*

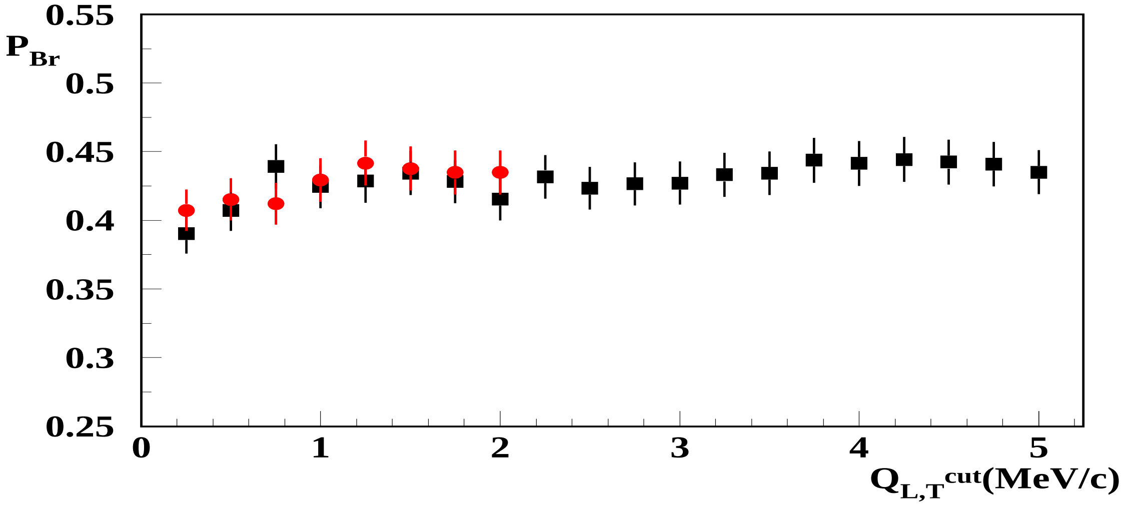

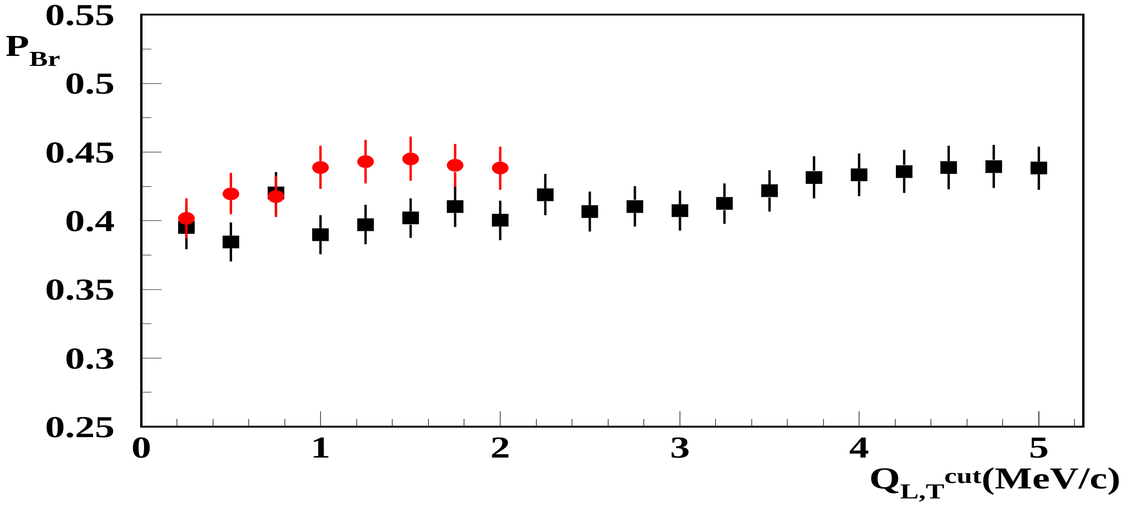

Fig. 8. *Pionium break-up probabilities determined from different choices of the upper limits ($Q^u_{T,L}$) in the rectangular integration domain to define the atom signal, for our results in this note (top) and for our previous results [1] (bottom). The coloured dots (red) show variations of Q^u_L holding $Q^u_T = 5MeV/c$ constant, whereas the black dots indicate variations of Q^u_T holding $Q^u_L = 2MeV/c$.*

3.5 Dependence on the Q_L upper limit

Our standard fit domain is the region $Q_L < 20MeV/c$ and $Q_T < 5MeV/c$, and the dependence of the P_{Br} with respect to the Q_L upper limit (Q_L^{up}) is analysed in table 6. We see how the P_{Br} fluctuates in a random way, with no appreciable systematics, and that the value at $Q_L^{up} = 20MeV/c$ is close to the average (P_{Br}=0.435).

Table 6
Values of break-up probability P_{Br} obtained from different choices of the upper limit (Q_L^{cut}) used to define the control region in Q_L projection.

$Q_L^{cut}(MeV/c)$	P_{Br}
22	0.430 ± 0.016
21	0.433 ± 0.016
20	0.435 ± 0.016
19	0.436 ± 0.016
18	0.437 ± 0.016
17	0.434 ± 0.016
16	0.440 ± 0.017
15	0.439 ± 0.017
14	0.435 ± 0.017
13	0.432 ± 0.017
12	0.433 ± 0.017
11	0.426 ± 0.017
10	0.430 ± 0.018

4 Momentum-dependent analysis

Following the approach of our earlier work [1], in this section we split the pair momentum spectrum in ten 600 MeV/c bins and perform independent fits at each momentum interval. The corrections applied are the same as for the global fit. The only change with respect to the latter is the choice of $0.5 \times 0.5(MeV/c)^2$ binsize, which is now obliged due to the strong statistics reduction at individual 2D bins. We use the same definition of β as in section 3.

4.1 Fit results

We present the final results after the introduction of all corrections, in order to avoid proliferation of figures. However, we keep record of the individual changes at each step, by giving the p-dependent and global fit results in the form of tables, distributed as follows:

- Table 7: The new Monte Carlo is used.
- Table 8: K^+K^- contamination is introduced, after the parametrization given in 1.
- Table 9: New Monte Carlo, K^+K^- contamination and target impurity correction.
- Table 10: In addition to the above, the finite-size correction is dropped.

Figures from 11 to 20 show the result of the 10 independent fits in the form of atom spectra (Q_L and Q_T) and break-up probabilities as function of Q_L and Q_T cuts.

The Pionium line-shape shows very good agreement between the prompt data signal and the Monte Carlo.

From table 11 we draw the same conclusions as from the global analysis. The introduccion of K^+K^- simulation improves the χ^2 by 5.2 units, and when the finite-size correction is removed, the χ^2 improves by 11.1 additional units. We consider this an indication that the latter should be done. Adding this two changes, the χ^2 is reduced by 16.3 units.

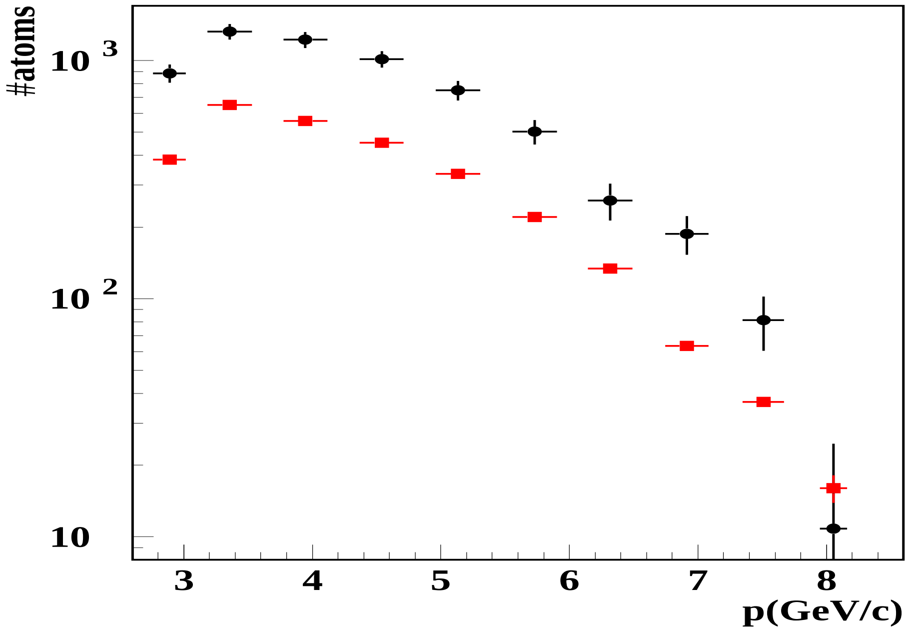

Fig. 9. *Fitted number of atom pairs as function of their lab-frame momentum (black circles) , as compared to the fitted number of Coulomb pais for* $Q_L > 2MeV/c$ *(coloured rectangles). The latter were normalized to half the area, to avoid the very large difference in actual scale.*

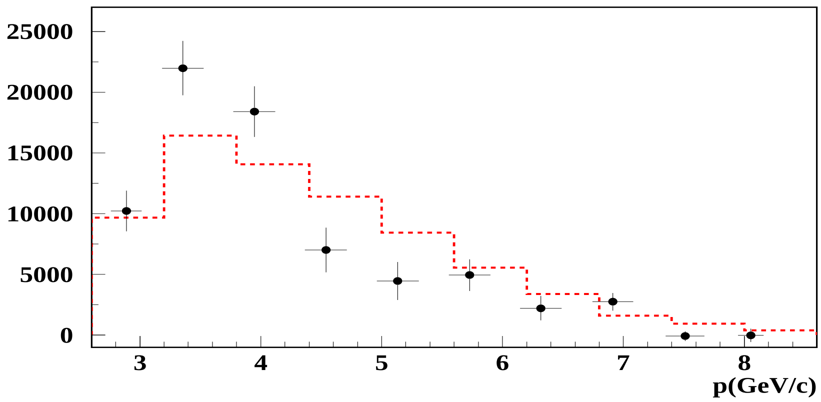

Fig. 10. *Fitted number of long-lifetime pairs (coloured), determined from* α_3 *parameter, as function of* $\pi^+\pi^-$ *momentum. It is compared with the number of Coulomb pairs shown in figure 9, normalized to the same area.*

Table 7
Results of the momentum-dependent fit, using correction a) only (see text). Break-up probability values P_{Br}, number of atom pairs N_A, α_1 and χ^2 over the entire fit region are indicated in this table, for every 600 MeV/c momentum interval p_i as defined in table 2.

	P_{Br}	N_A	α_1	χ^2 / ndf	χ_e^2 / ndf
p_1	0.417 ± 0.042	805. ± 73.	0.846 ± 0.015	312.8 / 360.	44.5 / 40.
p_2	0.395 ± 0.033	1265. ± 95.	0.819 ± 0.011	349.0 / 360.	48.0 / 40.
p_3	0.442 ± 0.038	1271. ± 97.	0.809 ± 0.012	360.1 / 360.	29.2 / 40.
p_4	0.490 ± 0.044	1183. ± 96.	0.853 ± 0.014	319.0 / 360.	50.7 / 40.
p_5	0.423 ± 0.044	789. ± 75.	0.856 ± 0.016	345.5 / 360.	26.2 / 40.
p_6	0.424 ± 0.055	546. ± 64.	0.824 ± 0.019	350.7 / 360.	35.3 / 40.
p_7	0.432 ± 0.083	346. ± 61.	0.837 ± 0.025	354.9 / 360.	32.5 / 40.
p_8	0.700 ± 0.146	269. ± 49.	0.752 ± 0.034	319.3 / 354.	67.3 / 40.
p_9	0.662 ± 0.156	143. ± 34.	0.852 ± 0.020	333.0 / 333.	48.1 / 40.
p_{10}	0.633 ± 0.587	65. ± 60.	0.847 ± 0.063	245.8 / 283.	46.5 / 40.

Table 8
Results of the momentum-dependent fit, using corrections a+b (see text). Break-up probability values P_{Br}, number of atom pairs N_A, α_1 and χ^2 over the entire fit region are indicated in this table, for every 600 MeV/c momentum interval p_i as defined in table 2.

	P_{Br}	N_A	α_1	χ^2 / ndf	χ_e^2 / ndf
p_1	0.414 ± 0.042	795. ± 72.	0.843 ± 0.015	312.9 / 360.	44.8 / 40.
p_2	0.390 ± 0.032	1237. ± 93.	0.814 ± 0.011	349.0 / 360.	48.5 / 40.
p_3	0.434 ± 0.037	1233. ± 94.	0.803 ± 0.012	360.0 / 360.	29.9 / 40.
p_4	0.478 ± 0.043	1136. ± 92.	0.845 ± 0.014	319.1 / 360.	50.0 / 40.
p_5	0.407 ± 0.043	744. ± 71.	0.846 ± 0.016	345.2 / 360.	24.9 / 40.
p_6	0.405 ± 0.053	509. ± 60.	0.812 ± 0.019	350.6 / 360.	34.3 / 40.
p_7	0.428 ± 0.083	332. ± 59.	0.823 ± 0.024	355.0 / 360.	31.7 / 40.
p_8	0.677 ± 0.143	251. ± 46.	0.739 ± 0.033	318.3 / 354.	66.2 / 40.
p_9	0.565 ± 0.144	119. ± 30.	0.852 ± 0.030	333.1 / 333.	48.4 / 40.
p_{10}	0.525 ± 0.631	53. ± 63.	0.847 ± 0.110	245.0 / 283.	46.4 / 40.

Table 9

Fit results of the momentum-dependent fit, using corrections a+b+c (see text). Break-up probability values P_{Br}, number of atom pairs N_A, α_1 and χ^2 over the entire fit region are indicated in this table, for every 600 MeV/c momentum interval p_i as defined in table 2.

	P_{Br}	N_A	α_1	χ^2 / ndf	χ^2_e / ndf
p_1	0.420 ± 0.042	795. ± 72.	0.843 ± 0.015	312.9 / 360.	44.8 / 40.
p_2	0.395 ± 0.033	1237. ± 93.	0.814 ± 0.011	349.0 / 360.	48.5 / 40.
p_3	0.440 ± 0.037	1233. ± 94.	0.803 ± 0.012	360.0 / 360.	29.9 / 40.
p_4	0.485 ± 0.044	1136. ± 92.	0.845 ± 0.014	319.1 / 360.	50.0 / 40.
p_5	0.413 ± 0.044	744. ± 71.	0.846 ± 0.016	345.2 / 360.	24.9 / 40.
p_6	0.411 ± 0.054	509. ± 60.	0.812 ± 0.019	350.6 / 360.	34.3 / 40.
p_7	0.434 ± 0.084	332. ± 59.	0.823 ± 0.024	355.0 / 360.	31.7 / 40.
p_8	0.686 ± 0.145	251. ± 46.	0.739 ± 0.033	318.3 / 354.	66.2 / 40.
p_9	0.573 ± 0.146	119. ± 30.	0.852 ± 0.030	333.1 / 333.	48.4 / 40.
p_{10}	0.533 ± 0.639	53. ± 63.	0.847 ± 0.110	245.0 / 283.	46.4 / 40.

Table 10

Final fit results of the momentum-dependent fit, using all corrections a+b+c+d (see text). Break-up probability values P_{Br}, number of atom pairs N_A, α_1 and χ^2 over the entire fit region are indicated in this table, for every 600 MeV/c momentum interval p_i as defined in table 2.

	P_{Br}	N_A	α_1	χ^2 / ndf	χ^2_e / ndf
p_1	0.430 ± 0.043	807. ± 72.	0.833 ± 0.014	311.8 / 360.	44.6 / 40.
p_2	0.406 ± 0.033	1260. ± 94.	0.804 ± 0.011	348.3 / 360.	48.6 / 40.
p_3	0.451 ± 0.038	1252. ± 95.	0.793 ± 0.012	359.3 / 360.	29.8 / 40.
p_4	0.495 ± 0.044	1151. ± 93.	0.835 ± 0.013	318.1 / 360.	50.0 / 40.
p_5	0.422 ± 0.044	755. ± 72.	0.837 ± 0.015	344.2 / 360.	24.8 / 40.
p_6	0.420 ± 0.055	516. ± 60.	0.803 ± 0.019	349.9 / 360.	34.3 / 40.
p_7	0.441 ± 0.085	334. ± 59.	0.814 ± 0.024	353.8 / 360.	31.6 / 40.
p_8	0.691 ± 0.145	251. ± 46.	0.731 ± 0.033	317.5 / 354.	66.0 / 40.
p_9	0.540 ± 0.141	113. ± 29.	0.852 ± 0.036	331.5 / 333.	48.3 / 40.
p_{10}	0.502 ± 0.646	50. ± 64.	0.847 ± 0.113	243.7 / 283.	46.2 / 40.

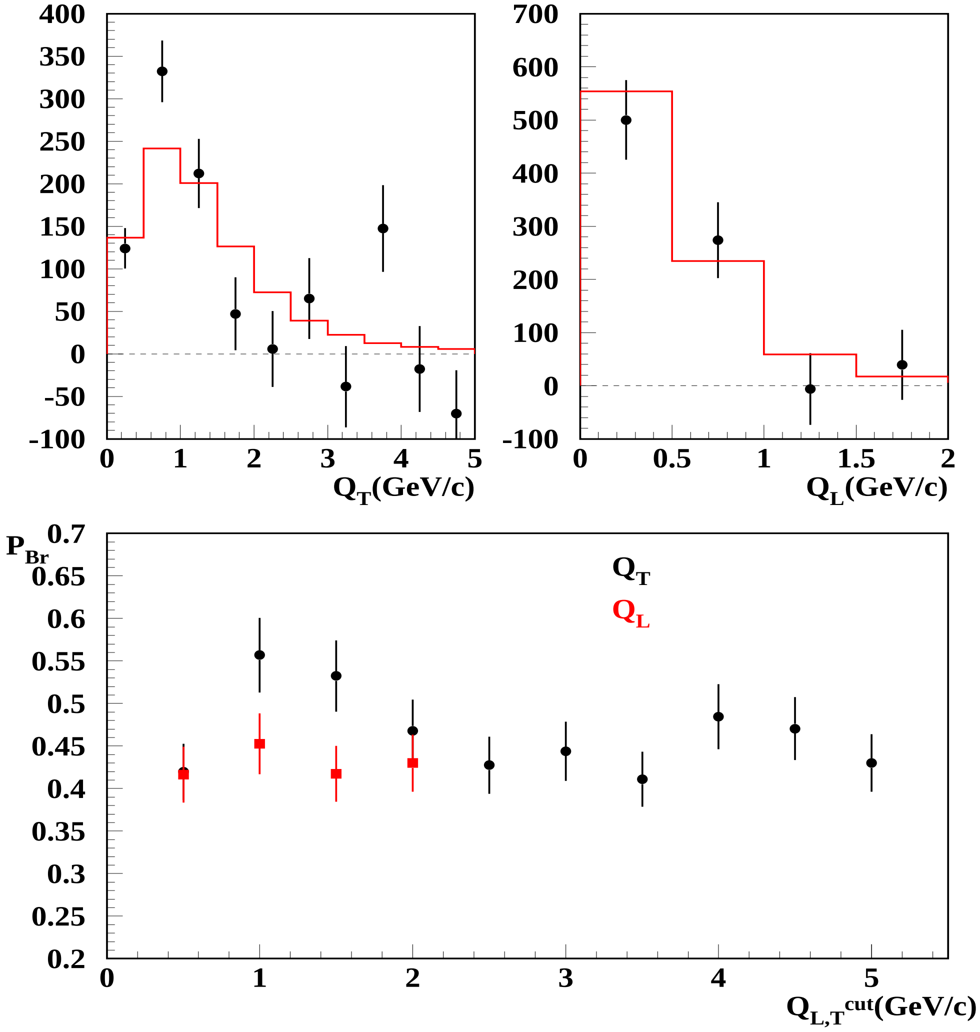

Fig. 11. *Fit results for the* $\pi^+\pi^-$ *momentum bin* $2.6 < p < 3.2$ GeV/c *in lab-frame.* Q_T *(top left) and* Q_L *(top right) projections of the atom signal found in the extrapolation region (*$Q_L < 2MeV/c$*) after subtraction of the Monte Carlo prediction with Pionium component removed. Values of break-up probability determined for different integration upper limits (*Q_T^u, Q_L^u*) to define the atom signal (bottom). Note the different* Q_L^u *values are all defined for* $Q_T^u = 5MeV/c$ *and* Q_T^u *values are defined for* $Q_L^u = 2MeV/c$*.*

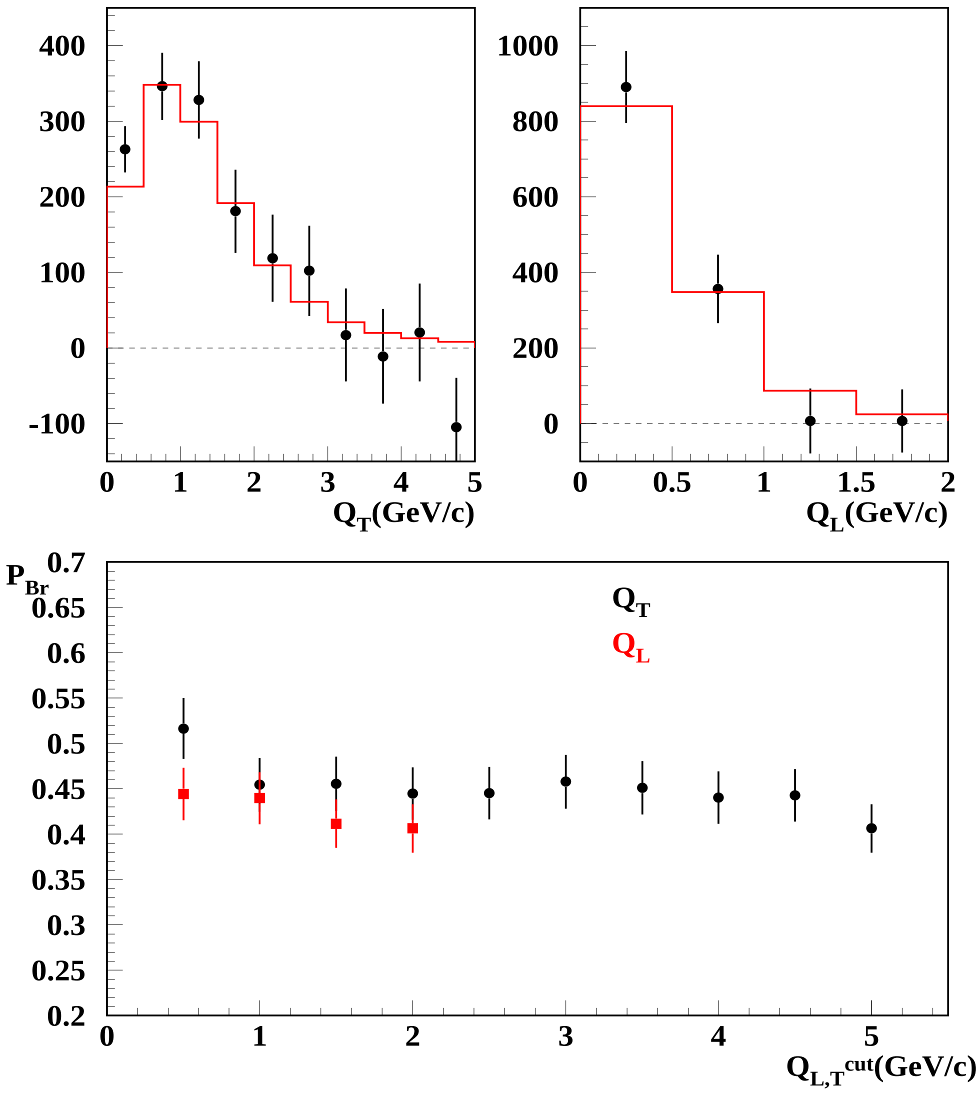

Fig. 12. *Fit results for the* $\pi^+\pi^-$ *momentum interval* $3.2 < p < 3.8$ *GeV/c in lab-frame. Caption is identical to figure 11 for the rest.*

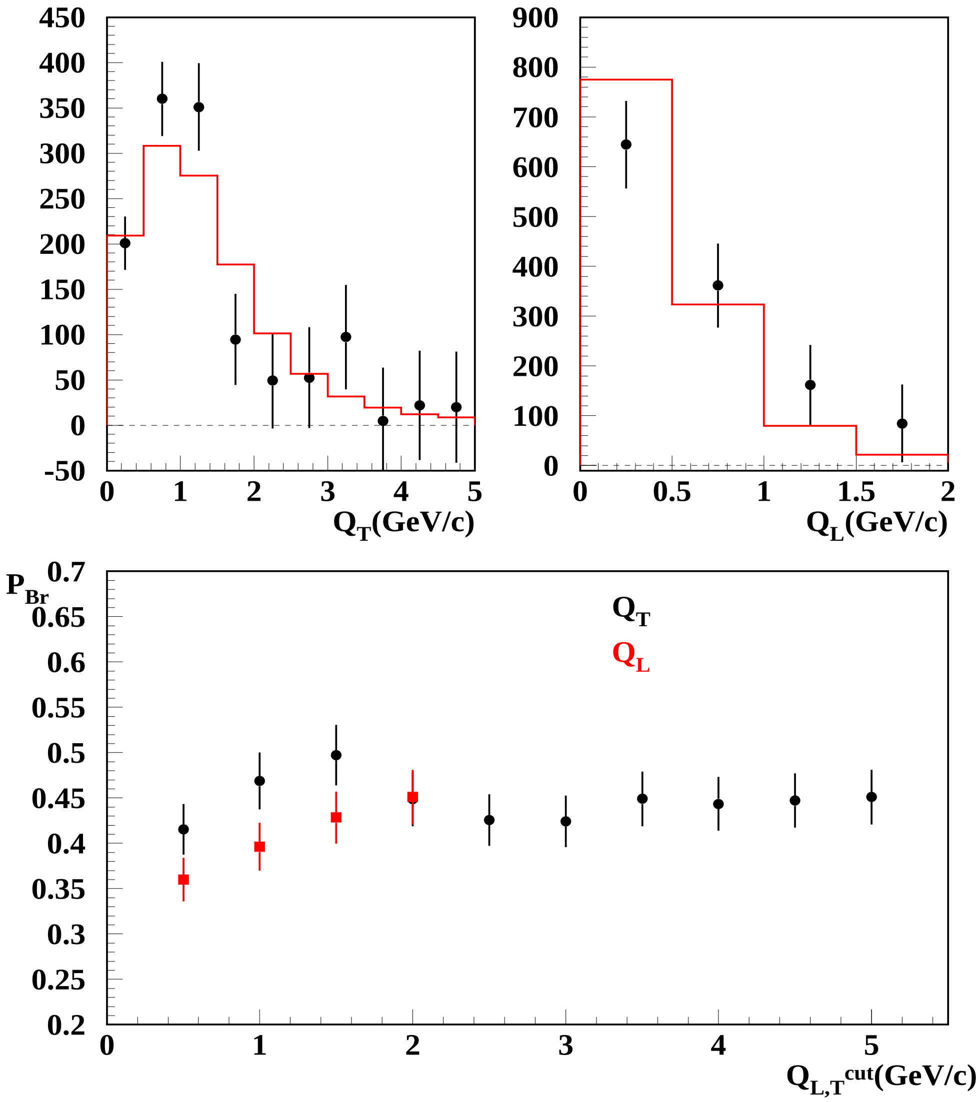

Fig. 13. *Fit results for the* $\pi^+\pi^-$ *momentum interval* $3.8 < p < 4.4$ *GeV/c in lab-frame. Caption is identical to figure 11 for the rest.*

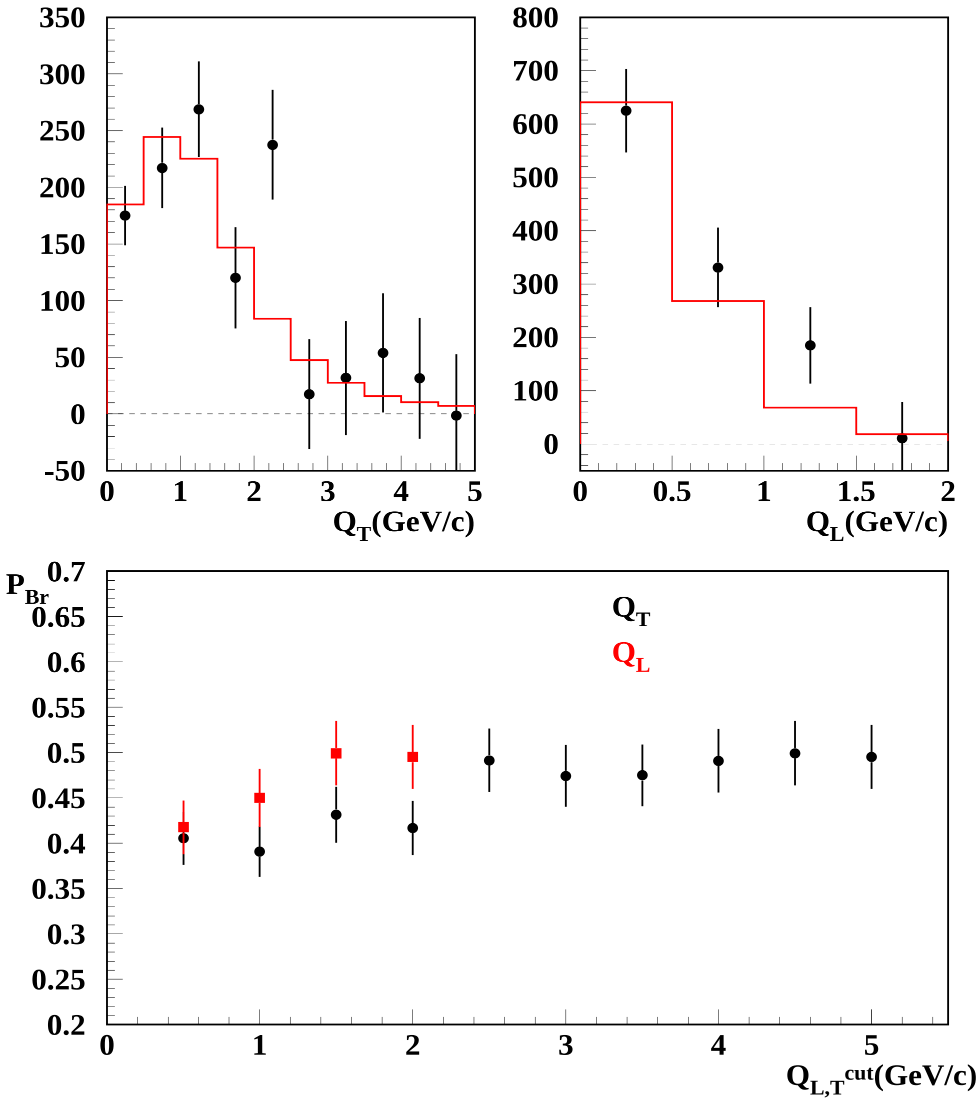

Fig. 14. *Fit results for the* $\pi^+\pi^-$ *momentum interval* $4.4 < p < 5.0$ *GeV/c in lab-frame. Caption is identical to figure 11 for the rest.*

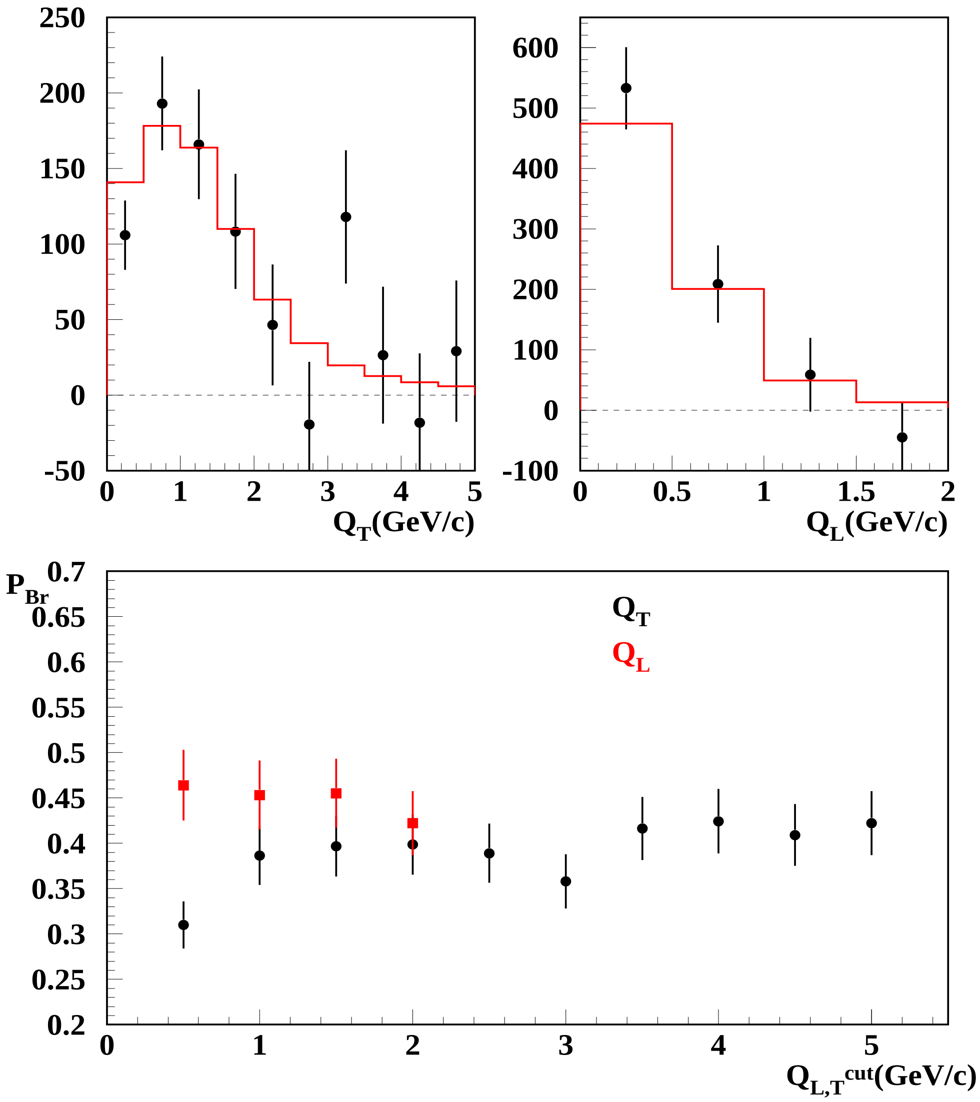

Fig. 15. *Fit results for the* $\pi^+\pi^-$ *momentum interval* $5. < p < 5.6$ *GeV/c in lab-frame. Caption is identical to figure 11 for the rest.*

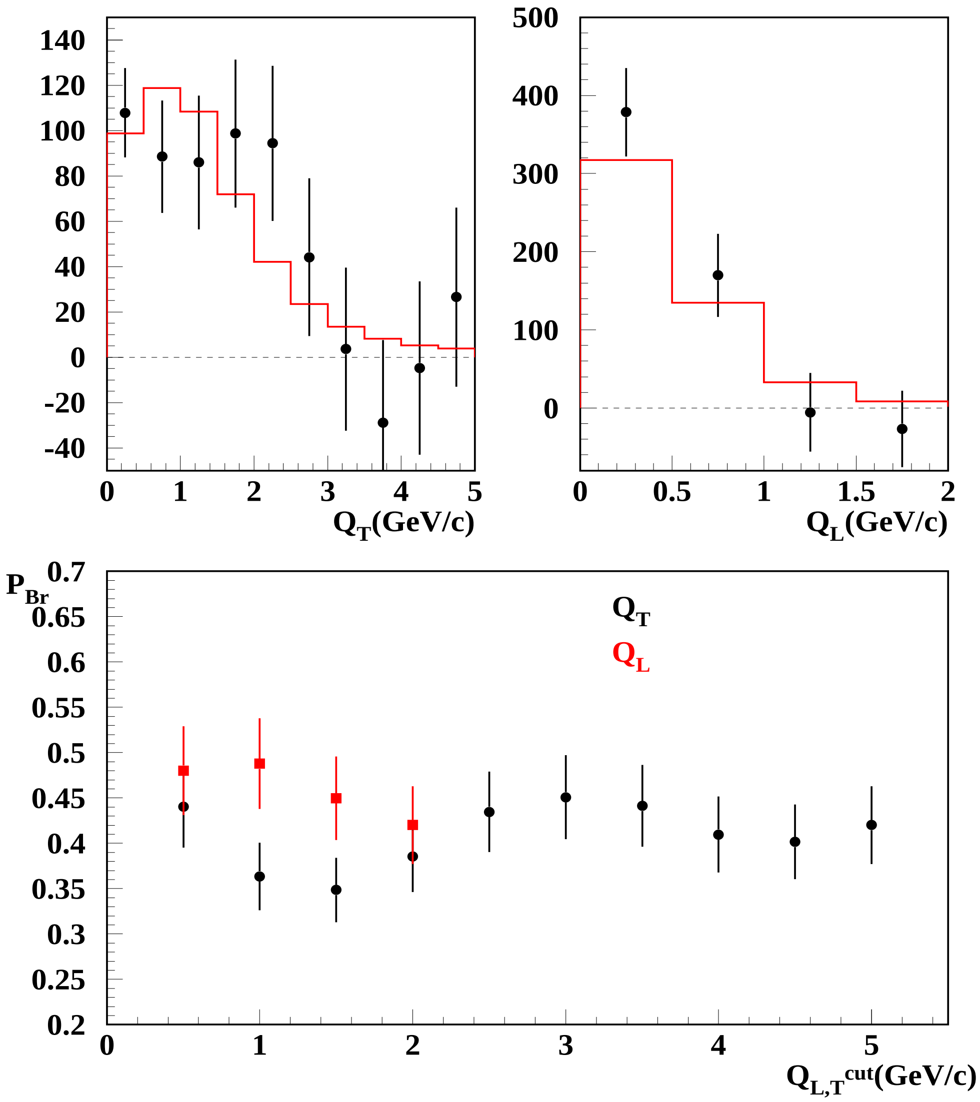

Fig. 16. *Fit results for the* $\pi^+\pi^-$ *momentum interval* $5.6 < p < 6.2$ *GeV/c in lab-frame. Caption is identical to figure 11 for the rest.*

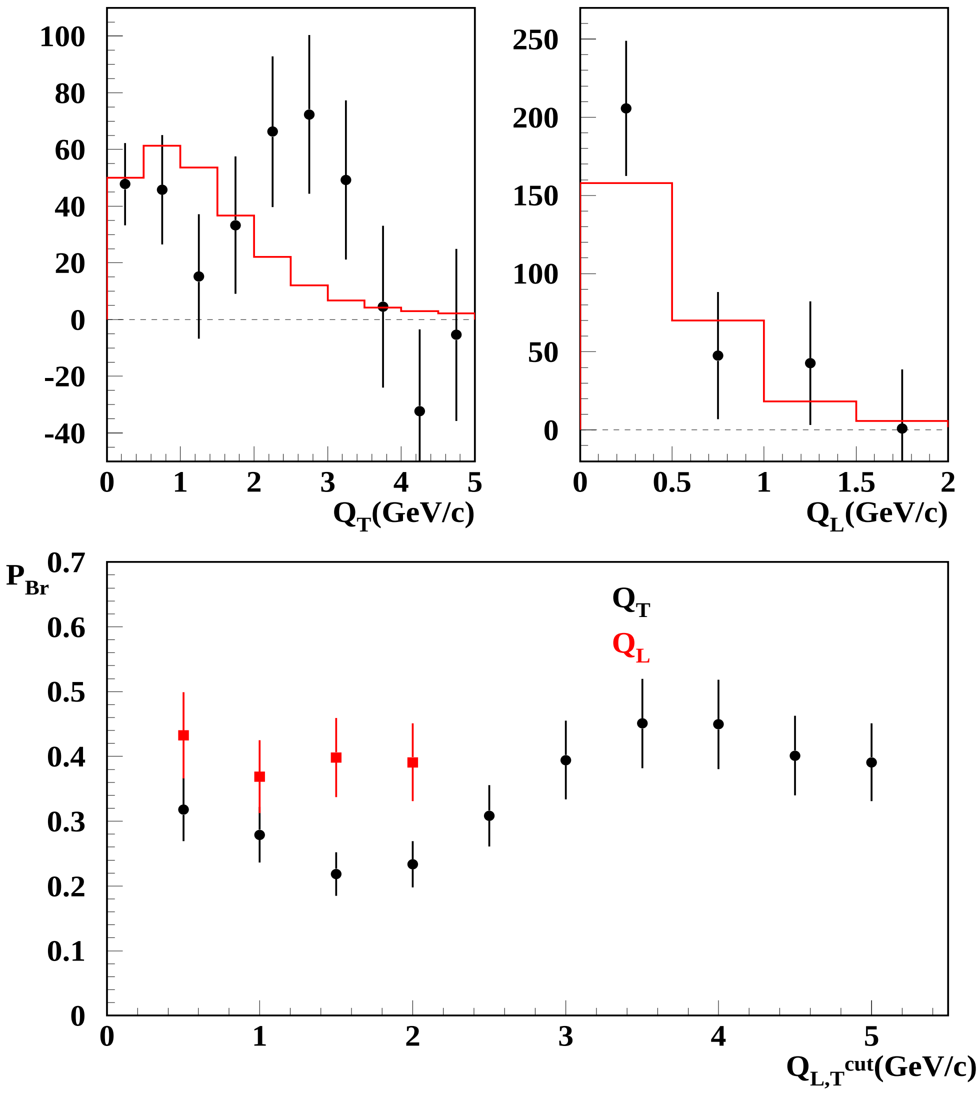

Fig. 17. *Fit results for the* $\pi^+\pi^-$ *momentum interval* $6.2 < p < 6.8$ *GeV/c in lab-frame. Caption is identical to figure 11 for the rest.*

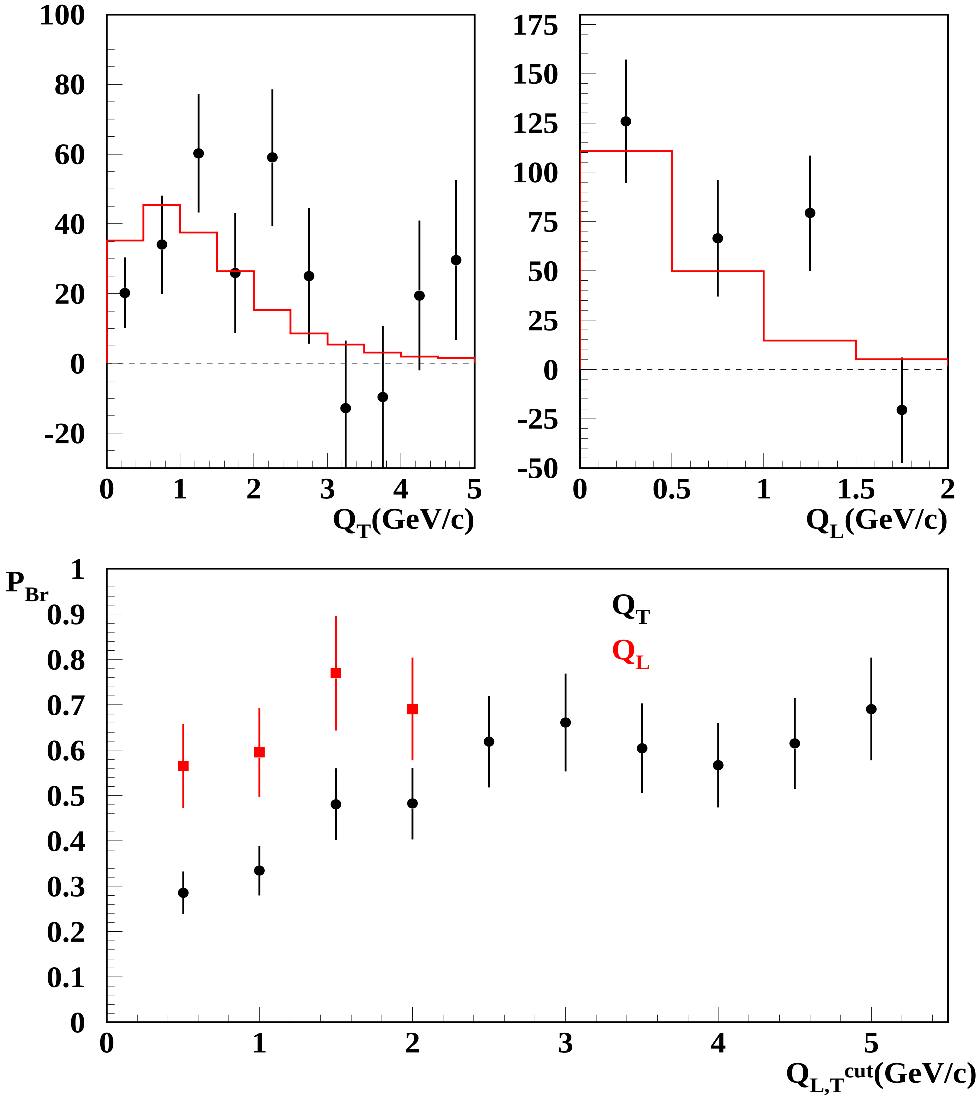

Fig. 18. *Fit results for the* $\pi^+\pi^-$ *momentum interval* $6.8 < p < 7.4$ *GeV/c in lab-frame. Caption is identical to figure 11 for the rest.*

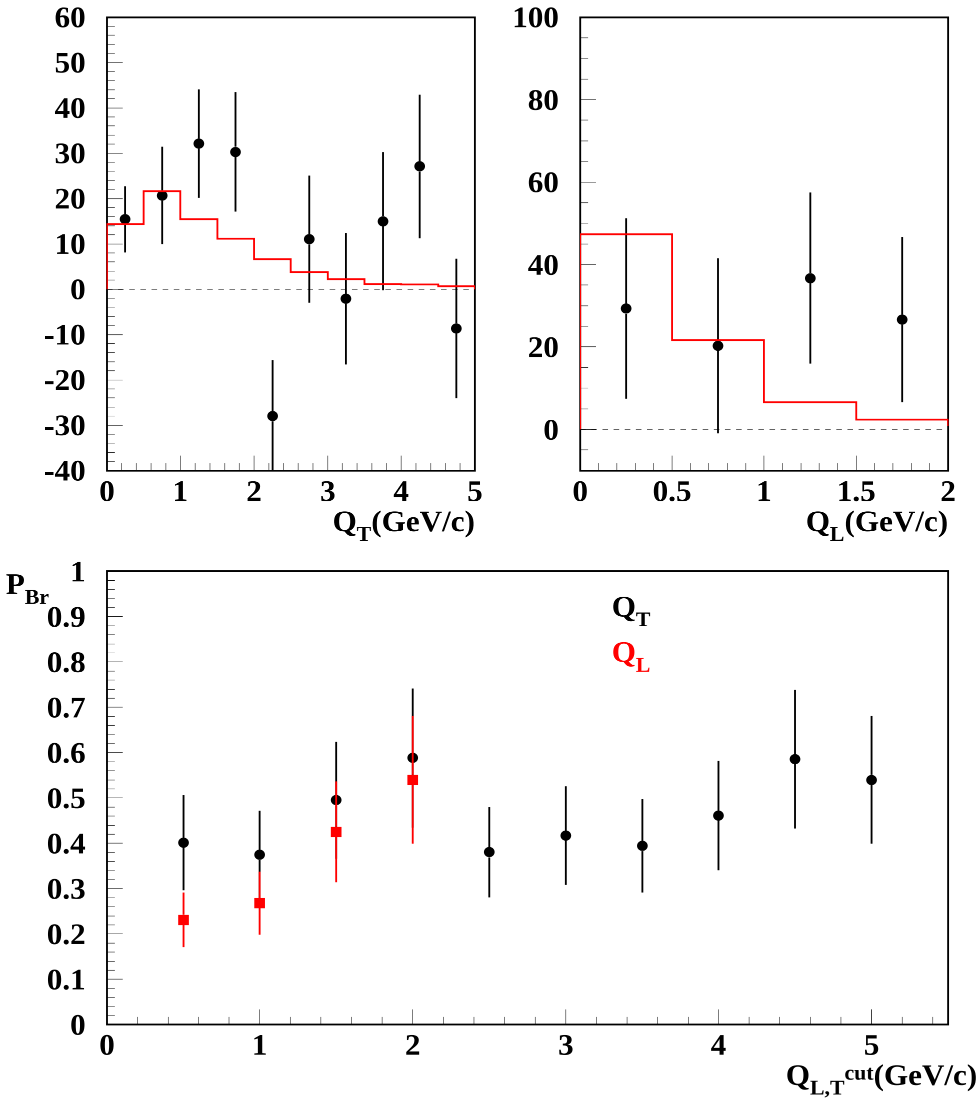

Fig. 19. *Fit results for the* $\pi^+\pi^-$ *momentum interval* $7.4 < p < 8.0$ *GeV/c in lab-frame. Caption is identical to figure 11 for the rest.*

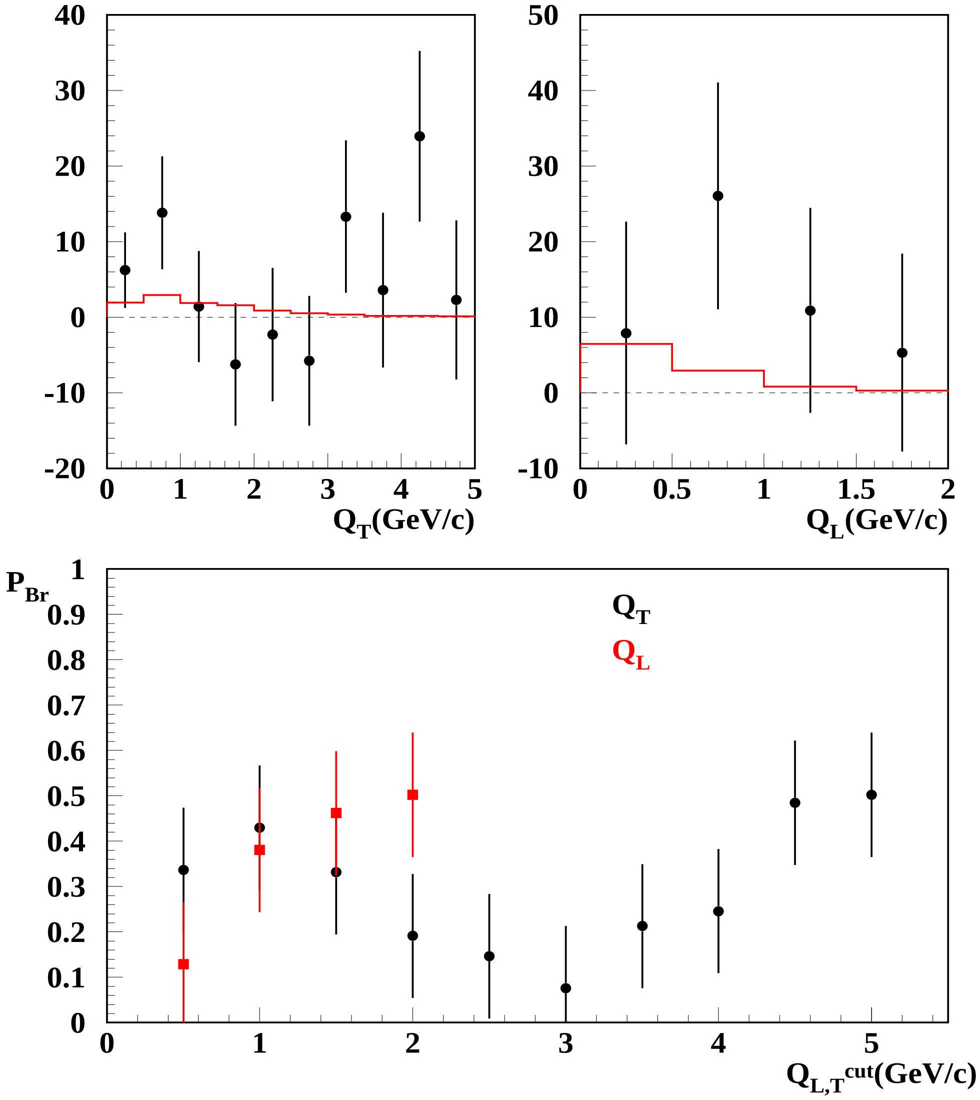

Fig. 20. *Fit results for the* $\pi^+\pi^-$ *momentum interval* $8.0 < p < 8.6$ *GeV/c in lab-frame. Caption is identical to figure 11 for the rest.*

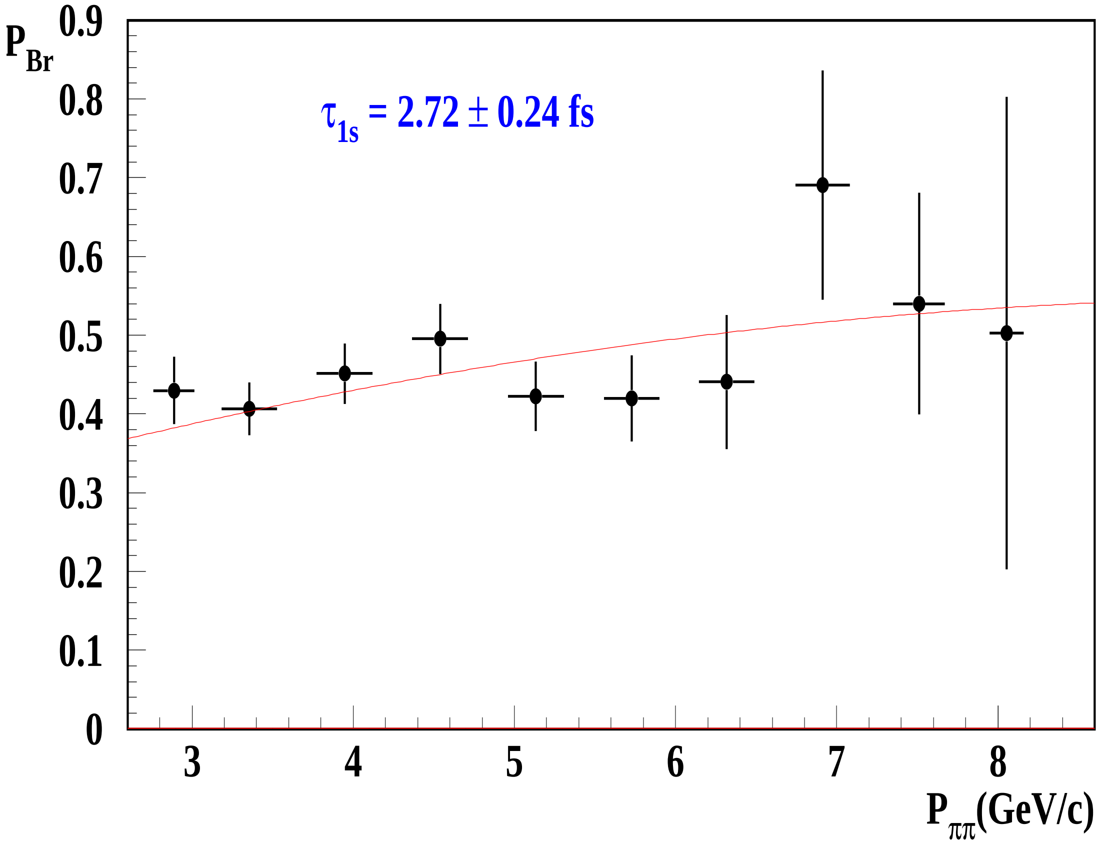

Fig. 21. *Pionium break-up probability P_{Br} as function of atom momentum, as compared to best fit Monte Carlo prediction with average Ni foil thickness. The fit χ^2 is 7.3 for 9 degrees of freedom. Pionium 1s lifetime value is indicated.*

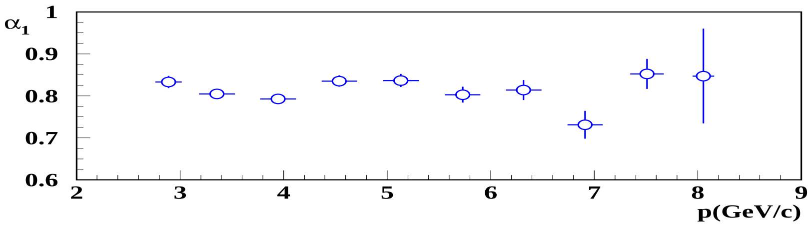

Fig. 22. *Fitted values of* α_1 *parameter as function of* $\pi^+\pi^-$ *momentum.*

Table 11
Momentum dependent fit

	A	A+B	A+B+C	A+B+C+D
χ^2	3718.5/3890	3713.3/3890	3713.3/3890	3702.2/3890
P_{Br}	0.433 ± 0.016	0.422 ± 0.016	0.428 ± 0.016	0.438 ± 0.016
N_A	6660 ± 230	6370 ± 223	6370 ± 223	6452 ± 224
N_C	732010 ± 4710	720987 ± 4662	720987 ± 4662	712522 ± 4618

The number of atom pairs N_A determined as function of p is plotted in figure 9 along with the number of Coulomb pairs given by the fit in each bin. Errors in N_A are given by MINOS variation of γ parameter. It is seen that atom production follows rather closely the spectrum of semi-inclusive $\pi^+\pi^-$ differential cross-section, as expected from bound state production. Please note that both of these spectra are uncorrected for spectrometer acceptance.

Pionium break-up probabilities can now be determined by using the momentum-dependent K-factors calculated in table 2, and they are shown in figure 21. Errors were propagated from those provided by the fit for N_A and N_C. P_{Br} values are compatible with a smooth increase with increasing atom momentum, as predicted by Monte Carlo tracking inside the target foil [9] [10]. We generate a continuous set of $P_{Br}(p)$ curves with varying values of the $1s$ Pionium lifetime (τ_{1s}). χ^2 minimization with respect to this set provides a measurement of τ_{1s} with an error.

The fitted values of α_1 parameter (fraction of Coulomb pairs) are also shown in figure 22 as function of p. They show a smooth behaviour.

In figure 10 we plot the remaining number of non-Coulomb pairs determined by the fit as function of p, after subtraction of accidentals (see [1]), and we compare the spectrum with that previously determined for Coulomb pairs (see figure 9).

5 Systematic error

As a consequence of the results presented in this note, we have re-evaluated the systematic error assesment with respect to our previous work.

We think that the error assigned to multiple scattering uncertainty can be further reduced, to the extent of being practically negligible. To illustrate this, in figure 23 we compare the reconstructed Pionium spectrum using our GEANT-DIRAC Monte Carlo with 15% increase of upstream radiation length (which corresponds to our 1.5% measurement [12]), to the Monte Carlo used in GEANT-DIRAC version 2.63, which is based upon a different radiation length hypothesis. The difference in both Q_L and Q_T appears to be insignificant, in terms of atom counting. Not only the multiple scattering in upstream detectors is known with 1.5% precision, but in addition the use of only the first planes of MSGC/GEM detectors in the final track fit [7] strongly decreases the multiple scattering uncertainty.

As far as the Q_L trigger acceptance is concerned, we have a new and more precise parametrization of it, as it has been seen the figure 2 and in table 6, and the error is reduced.

Simulation of the detector backgrounds, resolution and double ionization cuts (IH) are all known with high precision (see [1]), which is reflected in the small estimated systematic errors indicated in table 12.

The uncertainty of K^+K^- background is small, as a result of our previous measurement and the UrQMD Monte Carlo simulation. Moreover, the data show some sensitivity to this correction, in quantitative terms, as reported in section 3.2.

We had previously assigned a small contribution for the lack of precision in the atom line shape, which is mediated by multiple scattering, which is now dropped, taking into consideration that real prompt events are used to determine the atom signal.

Target impurity correction is not 100% known, because what we have are basically upper limits of contamination values. However, we believe an error of 30% of the correction is conservative. Only a chemical analysis of the bulk of the target foil would reduce this error to zero.

Assuming uncorrelated sources, we simulated random numbers with flat probability distributions within $\pm$ the extreme values indicated in table 12, each being added to the contribution of the previous one, and repeated this experiment many times. The output values show a fairly gaussian distribution with $\sigma = 0.006$, which can be used as a 1σ-equivalent estimator of the systematic error. However, we prefer to be more conservative and give a 1σ estimate $\Delta P_{br} = \pm 0.008$ for the systematic error.

Translation of ΔP_{Br} into $\Delta\tau_{1s}$ is done by means of the curve in figure 24.

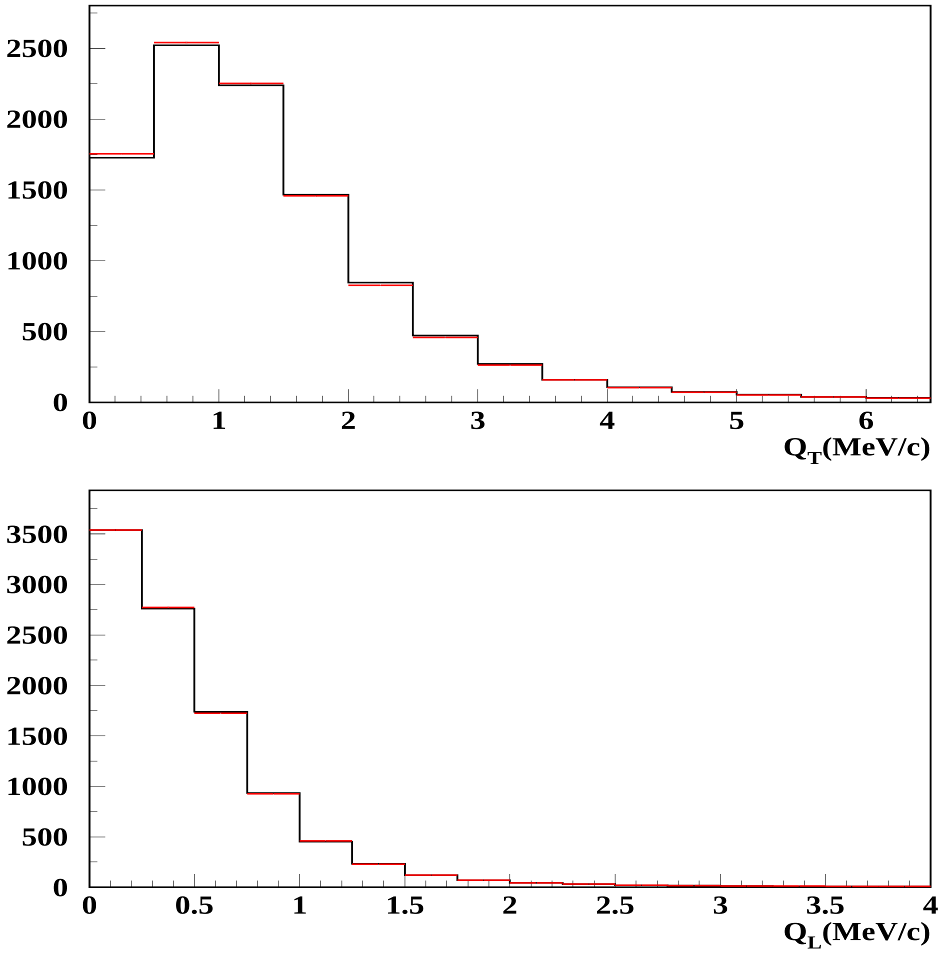

Fig. 23. *Comparison between the reconstructed Pionium Monte Carlo spectra using our GEANT-DIRAC version with increased* 15% *radiation length (black) and the GEANT-DIRAC version 2.63 (red).*

Table 12
Estimated contributions to systematic error in average break-up probability measurement. Last row indicates total systematic error equivalent to 1σ, under the assumption of uncorrelated effects.

Simulation error	ΔP_{Br} extreme values
Trigger acceptance	± 0.004
MSGC+SFD backgrounds	± 0.006
Double-track resolution	± 0.003
Double ionization cut	± 0.003
Target impurity	± 0.003
K^+K^- contamination	± 0.003
Total 1σ equivalent	± 0.006

6 Lifetime and $\pi\pi$ amplitude measurement

Our results can be summarized by saying that we have determined the Pionium break-up probability P_{Br} in the Ni foil in two different ways. One is making a global (momentum-integrated) fit, which provides a single measurement for the average P_{Br}, and another is making 10 independent experiments to measure this quantity in $600 MeV/c$ wide intervals of Pionium momentum. The results are in reasonable agreement with each other when the average P_{Br} values are compared, and have equal statistical errors. Both of them provide a very high fit quality with respect to the Monte Carlo hypothesis, in terms of χ^2 probability. From each of them we can determine the Pionium $1s$ lifetime, using the standard Pionium propagation code inside the foil.

Although our analysis strategy remains unchanged with respect to our earlier work, we have now a hopefully complete knowledge of all small corrections to the measurement where the magnitude and sign can be reliably evaluated.

We think that an optimal measurement can be chosen from the best global fit in table 5, with the systematic error estimated in section 5 :

$$P_{Br} = 0.435 \pm 0.016 \ (stat) \pm 0.008 \ (syst)$$

Using the relationship between P_{Br} and lifetime shown the figure 24, and obtained from the Pionium propagation code [9] [10], we determine the Pionium $1s$ lifetime:

$$\tau_{1S} = 2.63 \ {}^{+0.266}_{-0.255} \ (stat) \ {}^{+0.117}_{-0.111} \ (syst) \ fs$$

A quadrature of both sources of error yields the combined result :

$$\tau_{1S} = 2.63 \ {}^{+0.290}_{-0.278} \ fs$$

which can be converted into a measurement of the s-wave amplitude difference:

$$|a_2 - a_0| = 0.277 \ {}^{+\ 0.0153}_{-\ 0.0146} \ M_\pi^{-1} = (0.277 \pm 0.015) \ M_\pi^{-1}$$

by means of the expression [14]:

$$\Gamma_{1s} = \frac{1}{\tau_{1s}} = \frac{2}{9}\alpha^3 p \ |a_2 - a_0|^2 (1+\delta) \ M_\pi^2$$

where $\delta = (5.8 \pm 1.2) \times 10^{-2}$ and $p = \sqrt{M_{\pi+}^2 - M_{\pi 0}^2 - (1/4)\alpha^2 M_{\pi+}^2}$.

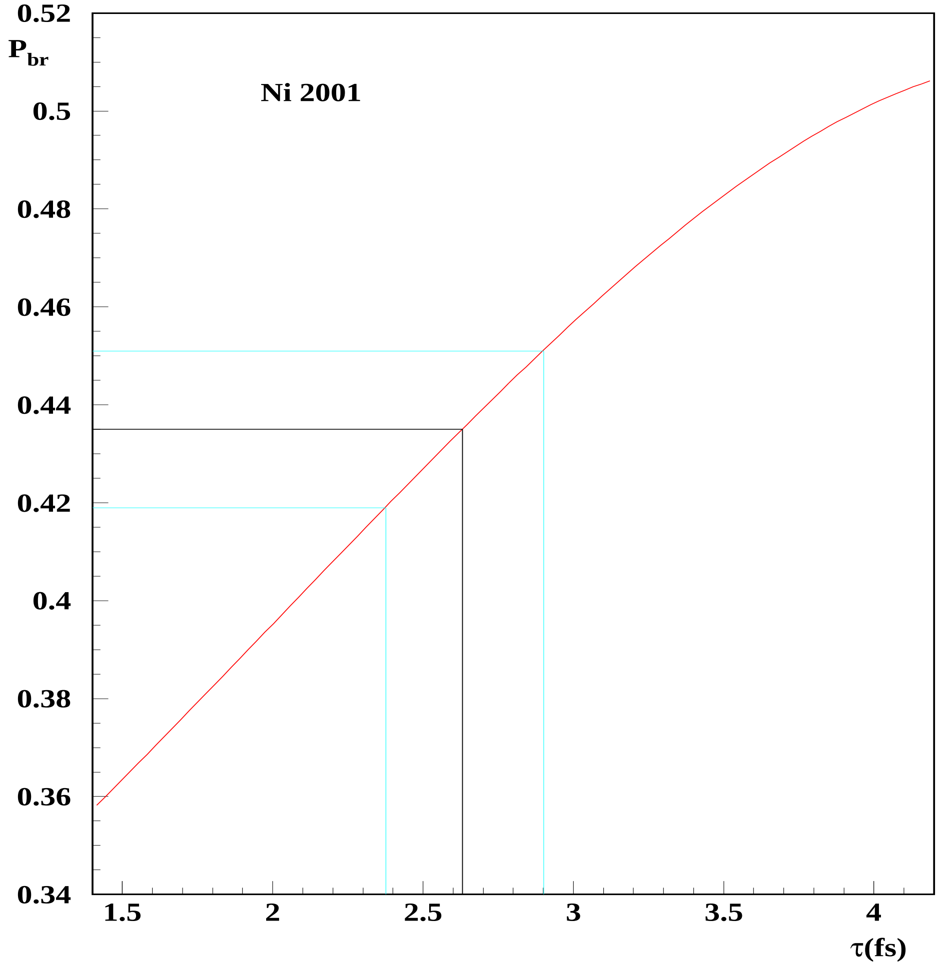

Fig. 24. *Parametrization of the dependence between break-up probability P_{Br} and lifetime for Pionium in the Ni target. A weighted average has been taken for the two slightly different thicknesses used in 2001 experiment.*

7 Acknowledgements

We thank Valeria Yazkov for useful comments about subtle aspects of momentum reconstruction in DIRAC, and particularly for having been so kind to cross-check our error analysis. We also acknowledge very warmly the support received from Cibrán Santamarina, in what concerns the utilization of his propagation code. Mikhail Zhabitsky has provided us useful advise for our pion pair simulation work, for which we thank him. We are also grateful to Catalina Petrascu for formulating proper questions and providing some ideas about corrections.

This publication would not have been possible without the strong support of Centro de Supercomputación de Galicia (CESGA), which we would like to thank here institutionally. The technical help received from J.J. Saborido Silva, who facilitated us the use of this strong computing network at USC, is also warmly appreciated. Our gratitude is extensive to Carlos Fernández Sánchez, in charge of the SVGD cluster at CESGA.

This work has been funded by the spanish National Program for Particle Physics from Ministerio de Educación y Ciencia (MEC), under projects FPA2005-06441, AEN99-0488 and AEN96-1671, and by Xunta de Galicia under projects PGIDIT06PXIB206100PR and PGIDT00PXI20602PR.

References

[1] DIRAC Note 06-03: Measurement of pionium lifetime, B.Adeva, A.Romero, O.Vazquez Doce.

[2] DIRAC Technical Proposal, B. Adeva et al., CERN/SPSLC 95-1 SPSLC/P 284, December 15, 1994 (see pag. 92)

[3] DIRAC note 06-05 : Experimental Measurement of a K^+K^- Signal at $p = 2.9 GeV/c$ in Ni 2001 Data, B. Adeva, A. Romero and O. Vázquez Doce.

[4] DIRAC note 07-02 : Study of $K^\pm\pi^\mp$, K^+K^- and K^-p production in DIRAC using time-of-flight measurements , B. Adeva, A. Romero and O. Vázquez Doce, C. Mariñas, J. L. Fungueiriño.

[5] UrQMD manual. http://th.physik.uni-frankfurt.de/˜ urqmd/
M. Bleicher et al., J. Phys. G25 (1999) 1859; hep-ph/9909407.

[6] DIRAC report "DIRAC targets", by A. Kuptsov, 5 March 2005.

[7] DIRAC Note 05-15: Full-Tracking Resolution in DIRAC with 2001 Data, B. Adeva, A. Romero and O. Vázquez Doce.
DIRAC Note 05-19: Addendum to Full-Tracking Resolution in DIRAC with 2001 Data, B. Adeva, A. Romero and O. Vázquez Doce.

[8] DIRAC note 04-06: Finite-size effects on two-particle production in continuous and discrete spectrum, R. Lednicky .

[9] DIRAC note 04-02: DIRAC events generator, C. Santamarina.

[10] C. Santamaria, M. Schuman, L.G. Afanasyev, T. Heim, A Monte-Carlo Calculation of the Pionium Breakup Probability with Different Sets of Pionium Target Cross Sections, J. Phys. B. At. Mol. Opt. Phys. 36 4273 (2003), arXiv:physics/0306161 v1.

[11] DIRAC Note 07-01: Parametrization of $\pi^+\pi^-$ pairs spectra at the DIRAC kinematic range,
M. Zhabitsky.

[12] DIRAC Note 05-16: Study of Multiple Scattering in Upstream Detectors in DIRAC, B. Adeva, A. Romero and O. Vázquez Doce.

[13] DIRAC Note 06-02: Evaluation of the measurement of multiple scattering for DIRAC set-up using standard DIRAC analysis tools, A. Benelli, D. Drijard, O. Gorchakov, L. Tauscher, V. Yazkov.

[14] J. Gasser et al., Phys. Rev. D 64 (2001) 016008, hep-ph/0103157.